Manuscript Details

Manuscript number	DES_2017_1492_R1
Title	Recovery of reactive MgO from reject brine via the addition of NaOH
Article type	Full Length Article

Abstract

Reject brine, generated as a waste at the end of the desalination process, presents a useful source for the extraction of valuable resources. This study investigated the recovery of reactive MgO from reject brine obtained from a local desalination plant. This was enabled via the reaction of Mg2+ present within reject brine with an alkali source (NaOH), which led to the precipitation of Mg(OH)2, along with a small amount of CaCO3. The determination of the optimum NaOH/Mg2+ ratio led to the production of the highest amount of yield. The synthesized Mg(OH)2 was further calcined under a range of temperatures (500-700 °C) and durations (2-12 hours) to produce reactive MgO. A detailed characterization of MgO obtained under these conditions was presented in terms of its reactivity, specific surface area (SSA), composition and microstructure. While an increase in the calcination temperature and duration decreased the reactivity and SSA of MgO, samples calcined at 500 °C for 2 hours revealed the highest reactivity, which was reflected by their SSA of 51.4 m2/g.

Keywords	Reject brine; reactive MgO; NaOH; Mg(OH)2; calcination

Corresponding Author	En-Hua Yang
Corresponding Author's Institution	Nanyang Technological University
Order of Authors	Haoliang Dong, Cise Unluer, En-Hua Yang, Abir Al-Tabbaa
Suggested reviewers	Fei Jin, Martin Liska, Liwu Mo

Submission Files Included in this PDF

File Name [File Type]

DES R1_Reject brine MgO NaOH_Cover.docx [Cover Letter]

DES R1_Reject brine MgO NaOH_Response .docx [Response to Reviewers]

DES R1_Reject brine MgO NaOH_Manu marked.doc [Revised Manuscript with Changes Marked]

DES R1_Reject brine MgO NaOH_Highlight.docx [Highlights]

DES R1_Reject brine MgO NaOH_Manu.doc [Manuscript File]

To view all the submission files, including those not included in the PDF, click on the manuscript title on your EVISE Homepage, then click 'Download zip file'.

Recovery of reactive MgO from reject brine via the addition of NaOH

Haoliang Dong[a], Cise Unluer[a], En-Hua Yang[a,*], Abir Al-Tabbaa[b]

[a] School of Civil and Environmental Engineering, Nanyang Technological University, 50 Nanyang Avenue, Singapore 639798, Singapore

[b] Department of Engineering, University of Cambridge, Trumpington Street, Cambridge CB2 1PZ, UK

Abstract

Reject brine, generated as a waste at the end of the desalination process, presents a useful source for the extraction of valuable resources. This study investigated the recovery of reactive MgO from reject brine obtained from a local desalination plant. This was enabled via the reaction of Mg^{2+} present within reject brine with an alkali source (NaOH), which led to the precipitation of $Mg(OH)_2$, along with a small amount of $CaCO_3$. The determination of the optimum $NaOH/Mg^{2+}$ ratio led to the production of the highest amount of yield. The synthesized $Mg(OH)_2$ was further calcined under a range of temperatures (500-700 °C) and durations (2-12 hours) to produce reactive MgO. A detailed characterization of MgO obtained under these conditions was presented in terms of its reactivity, specific surface area (SSA), composition and microstructure. While an increase in the calcination temperature and duration decreased the reactivity and SSA of MgO, samples calcined at 500 °C for 2 hours revealed the highest reactivity, which was reflected by their SSA of 51.4 m^2/g.

Keywords: Reject brine; reactive MgO; NaOH; $Mg(OH)_2$; calcination

* Corresponding author. Address: N1-01b-56, 50 Nanyang Avenue, Singapore 639798. Tel.: +65 6790 5291; fax: +65 6791 0676. *E-mail:* ehyang@ntu.edu.sg

1 Introduction

Magnesium oxide (MgO) finds use in various applications ranging from the refractory industry to agriculture, chemical and environmental applications [1-4]. Another increasingly popular use of reactive MgO was reported in the construction industry as an expansive additive [5] and as a novel binder in the development of concrete formulations [6-11]. While the majority of MgO produced today is obtained through the processing of naturally occurring minerals such as magnesite ($MgCO_3$) [3], around 14% of the global MgO supply is from the calcination of magnesium hydroxide ($Mg(OH)_2$) synthesized from seawater or magnesium-rich brine sources. The synthetic MgO obtained from seawater/brine demonstrates a higher purity and reactivity compared with MgO produced through the calcination of magnesite [12]. MgO that possesses higher purity and specific surface area (SSA) is widely used in high-end pharmaceutical and semiconductor applications as an additive or a catalyst [1-4].

The recovery of brucite ($Mg(OH)_2$) from seawater/brine deploys the use of a strong base to precipitate Mg^{2+} from the solution. During this process, it is essential to reach an appropriate pH level in order to form the precipitates. Previous studies [13, 14] have shown that the ideal pH for the formation of carbonates is above 9, which favors the transformation of carbon dioxide and bicarbonates to CO_3^{2-}. The pH level of gelatinous $Mg(OH)_2$ could be even higher due to the requirement of surplus hydroxide. These trends were also confirmed by [15], who demonstrated the occurrence of the precipitation process at a pH of 8.5, whereas higher pH values led to increased brucite formation.

Lime (CaO) [16] or dolomite lime (CaO·MgO) [17] are used as a base during the synthesis of $Mg(OH)_2$ from seawater. The use of dolomite lime reduces the amount of seawater/brine

needed for the production of the same amount of MgO obtained via the use of CaO because dolomite lime itself contains MgO. However, the uses of these Ca-bearing bases often lead to the precipitation of Ca-based compounds (e.g. $CaCO_3$) and thus reduce the purity and content of Mg-based precipitates. Furthermore, the Ca-bearing bases can react with sulphate (SO_4^{2-}) present in the solution to form gypsum ($CaSO_4 \cdot 2H_2O$), which may necessitate the pre-treatment of the solution through the addition of $CaCl_2$ to remove sulphate in seawater/brine.

Apart from Ca-based bases, several studies have suggested the use of other alkali sources to precipitate Mg^{2+} from seawater/brine [15, 18-23]. $NaCO_3$ and NaOH were reported to recover Ca and Mg from mining and seawater desalination brines. Recovery ratios higher than 94-96 % of Ca were achieved for pH higher than 10 via the use of $NaCO_3$ and recovery ratios higher than 97-99 % of Mg were achieved for pH higher than 11 via the addition of NaOH [23]. Another proposed additives was sodium hydroxide (NaOH) along with oxalic acid, which produce magnesium oxalate (MgC_2O_4) from brine. Previous studies [21] demonstrated the selective precipitation of Mg- and Ca-oxalate at different pH values. Ca-oxalate was first precipitated and removed at an oxalate/Ca molar ratio of 6.82 at a pH of < 1. This was followed by the precipitation of Mg^{2+} from the brine residue at a NaOH/oxalate/Mg ratio of 3.21:1:1.62 at a pH range of 3-5.5, leading to a high yield of pure magnesium oxalate.

These steps can be followed by the production of reactive MgO via the calcination of Mg-containing precipitates, such as magnesium hydroxide and magnesium oxalate. Numerous studies have been carried out to characterize MgO obtained from different sources [12, 24-32]. The outcomes of these studies have identified the main factors that influence the properties of MgO produced through the dry route (i.e. decomposition of magnesite) as the calcination conditions (i.e. temperature and residence time). Accordingly, increased

calcination temperatures and/or prolonged durations lead to the agglomeration of MgO particles due to sintering, which decreases the porosity and reactivity of MgO [30].

Desalination provides an alternative means to meet the residential and industrial water demands in water-stressed countries like Singapore [33, 34]. Currently, the two desalination plants in Singapore provide 100 million gallons (448,500 m^3) of drinking water on a daily basis, which can meet 25% of Singapore's current water demand. With three additional desalination plants being built, the five desalination plants are designed to provide a total of 190 million gallons (852,150 m^3) of water per day by 2020 [35]. On a global level, the daily production level of desalinated water by 18,426 desalination plants exceeds 86.8 million cubic meters [36]. Production of desalinated water generates an almost equal amount of reject brine [20], a high salt concentration waste by-product produced at the end of the desalination process [37]. Reject brine is often discharged directly back into sea, which threatens the marine life and ecosystem by altering the local flora and fauna due to its high salinity [38]. Therefore, the disposal and management of reject brine remains a major challenge as well as an environmental threat [38, 39], which can pave the way for its use in the recovery of valuable metals and useful solids instead of direct discharge [40].

The desalination process involves the addition of a variety of chemicals to enable the precipitation of the colloidal particles before running through the filtration process. Therefore, the resulting reject brine contains a very high concentration of dissolved salts and suspended constituents, creating variations in its composition in comparison to seawater, natural brine or synthetic solutions. While previous studies [15, 18-22] have reported the synthesis of MgO or its derivatives from seawater, natural brine or synthetic solutions, this study aims to explore the feasibility of the recovery of Mg^{2+} from reject brine collected from

a local desalination plant. The proposed method involves the addition of NaOH, which serves as a pH adjuster and controls the pH of the solution. Unlike Ca-bearing bases, which often lead to the precipitation of a Ca-based compound (e.g. $CaCO_3$) along with Mg-phases, the use of NaOH can increase the purity of Mg-based precipitates. Furthermore, when compared with other bases (e.g. NH_4OH, KOH and Na_2CO_3), NaOH possesses other advantages in terms of health and safety, cost effectiveness and base strength it provides [31].

This research presents a comprehensive study on the synthesis of $Mg(OH)_2$ and production of reactive MgO from reject brine via the use of NaOH. The key parameters affecting the properties of the synthesized $Mg(OH)_2$ and its calcination to produce reactive MgO were investigated. Several techniques were utilized to characterize the synthesized $Mg(OH)_2$ and MgO including inductively coupled plasma-optical emission spectroscopy (ICP-OES), X-ray powder diffraction (XRD), field emission scanning electron microscopy (FESEM), thermogravimetric and differential thermal analysis (TG/DTA), Brunauer-Emmett-Teller (BET) analysis and acid neutralization. Production cost of reactive MgO from reject brine via the addition of NaOH was calculated to evaluate the economic feasibility of the approach. Results obtained at the end of this study were used to demonstrate the use of reject brine as an alternative source for the recovery of MgO with a high reactivity.

2 Materials and Methodology

2.1 Materials

Reject brine was collected and sampled from a local desalination plant in Singapore, which adopts a reverse osmosis (RO) membrane system to purify saline water and produce drinkable water for human use. These membranes reject more than 99.5% of the dissolved

salts and suspended materials in the feedwater, resulting in a highly concentrated reject waste stream which contains suspended constituents and a 2- to 7-fold increased concentration of dissolved salts [33, 34, 41]. Prior to any analysis, the reject brine was first filtrated through a 45 μm membrane filter to remove the large suspended solids. The pH of reject brine as received was around 8.0. The chemical composition of the reject brine, obtained via inductively coupled plasma-optical emission spectroscopy (ICP-OES) and ion chromatography (IC), is summarized in Table 1. Along with Mg^{2+}, which was present at a concentration of 1718 ppm, other impurities such as Na^{+}, K^{+} and Ca^{2+} were also identified in the reject brine. Sodium hydroxide (NaOH, reagent grade, pellets) supplied by VWR Pte Ltd in Singapore, was used as the alkaline base in the current study.

Table 1 Chemical composition of the reject brine used in this study

Element	Cl	Na	SO_4	Mg	K	Ca	Sr	B	Si	Li	P	Al
Concentration (ppm)	55243	13580	4423	1718	845.7	471.3	14.6	3.8	3.7	0.3	0.2	0.1

2.2 Methodology

Different amounts of NaOH solution (16 M) were added into 200 ml of reject brine to study the influence of $NaOH/Mg^{2+}$ molar ratio (ranging from 2 to 4) on the recovery of Mg^{2+}. NaOH solution was added into reject brine at once and the initial pH of solution was recorded. The solution was mixed at constant speed of 300 rpm by a magnetic stirrer at room temperature (25 °C). A pH/thermometer probe was used to monitor and record the temperature and pH of the reaction in the solution. Experiment was terminated when the pH of the solution stabilized. The solids were separated from the residual brine through a centrifuge. After the solids were collected, they were re-dispersed and washed thoroughly by ultra-pure water in an ultrasonic bath to remove surface-attached ions. The washed solids were separated from the solution through a centrifuge. This washing process was repeated for

three times to remove surface-attached ions and soluble salts. The washed solids were then oven-dried at 105 °C for 24 hours to remove free water before grinding into powder form. The ground samples were calcined at pre-determined temperatures (500-700 °C) and durations (2-12 hours) in an electric furnace to produce reactive MgO.

Several techniques were utilized to characterize the synthesized $Mg(OH)_2$ and MgO. X-ray powder diffraction (XRD) was performed via a Bruker D8 Advance with a Cu Kα source under the operation conditions of 40 kV and 40 mA, emitting radiation with a wavelength of 1.5405 angstroms, scan rate of 0.02 °/step, and a 2θ range of 5 to 70°. A JSM-7600F thermal field emission scanning electron microscopy (FESEM) was used to analyze the microstructure of the solids by imaging powder surface. The decomposition of each sample was studied via thermogravimetric and differential thermal analysis (TG/DTA) using a PyrisDiamond TGA 4000 operated at a heating rate of 10 °C/min under air flow. The specific surface area (SSA) of the synthesized samples was obtained by Brunauer-Emmett-Teller (BET) analysis from nitrogen adsorption-desorption isotherms using a Quadrasorb Evo automated surface area and pore size analyser. The reactivity of MgO was measured by acid neutralization, during which 0.28 grams of the synthesized MgO was added into 50 ml of 0.07 mol/L citric acid solution along with phenolphthalein (i.e. pH indicator). The neutralization time was measured and reported as an indicator of reactivity [3, 30].

Economic feasibility of the production of reactive MgO from reject brine in this study was evaluated and compared with other production routes. The total cost of the production of reactive MgO from reject brine mainly consists of the raw material cost for synthesis (e.g. NaOH) and the energy cost during calcination. Reject brine is the waste water produced at the end in the desalination plant, and thus the material cost and energy cost of reject brine are

assumed to be zero. Transportation of raw materials and the grinding and packing of reactive MgO products are not considered into the calculation since they do not contribute significantly to the overall process.

3 Results and Discussion

3.1 Recovery of Mg^{2+} and Ca^{2+} from reject brine

The formation of $Mg(OH)_2$ was observed via the reaction between the Mg^{2+} in the reject brine and OH^- provided by NaOH. The addition of NaOH also enabled the conversion of HCO_3^-, present in the reject brine, to CO_3^{2-}. This led to a reaction of CO_3^{2-} with Ca^{2+} and resulted in the precipitation of $CaCO_3$. The reaction paths observed during this process are shown in Equations 1-4 below.

$$NaOH_{(aq)} \rightarrow Na^+ + OH^- \quad (1)$$

$$Mg^{2+} + 2OH^- \leftrightarrow Mg(OH)_2 \quad (2)$$

$$NaOH_{(aq)} + HCO_3^- \leftrightarrow CO_3^{2-} + Na^+ + H_2O \quad (3)$$

$$Ca^{2+} + CO_3^{2-} \leftrightarrow CaCO_3 \quad (4)$$

The kinetics of the reaction between reject brine and NaOH reflected by the change of pH are summarized in Figure 1. A rapid reaction was observed, which was completed in less than 30 minutes as the pH reached an equilibrium state. The pH increased with the molar ratio of $NaOH/Mg^{2+}$. This was due to the increased concentration of OH^- provided by the higher amounts of NaOH introduced into the solution, whereas a smaller increase was observed at $NaOH/Mg^{2+}$ ratios of > 2.5.

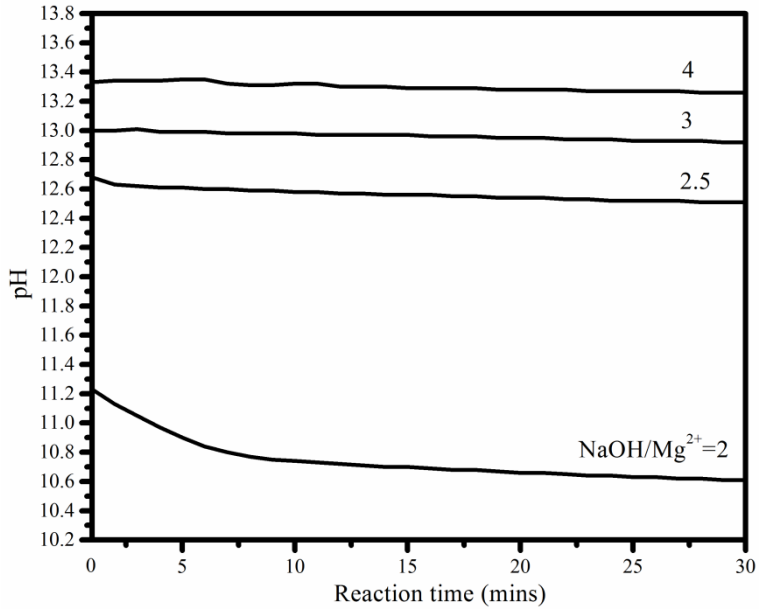

Figure 1 pH of the reaction between reject brine and NaOH at different $NaOH/Mg^{2+}$ ratios

Figure 2 shows the recovery rate of Mg^{2+} and Ca^{2+} in weight percentage after the reaction of reject brine with NaOH. As can be seen, the recovery rates for both Mg^{2+} and Ca^{2+} increased with increasing $NaOH/Mg^{2+}$ molar ratio, which achieved a similar recovery level of 94-99% of Mg as reported in [23]. The recovered Mg^{2+}/Ca^{2+} ratio was used as an indication of the purity level of the resulting $Mg(OH)_2$ precipitates. As shown in Figure 2, Mg^{2+}/Ca^{2+} was highest (19.6) at a $NaOH/Mg^{2+}$ ratio of 2 and decreased with increasing $NaOH/Mg^{2+}$ ratio. This was because at a $NaOH/Mg^{2+}$ molar ratio of 2, the ion product in the solution ($[Mg^{2+}][OH^-]^2 = 7\times10^{-8.6}$ $mol^3\ l^{-3}$, pH = 11.2) was larger than the solubility product constant of $Mg(OH)_2$ (1.8×10^{-11} $mol^3\ l^{-3}$) [42]. The supersaturation condition enabled the reaction between OH^- and Mg^{2+} and the formation of $Mg(OH)_2$. Furthermore, pH increased with increasing $NaOH/Mg^{2+}$, which provided excessive OH^- in the solution to attack HCO_3^-. This caused in a shift in Equation 3 towards the right hand side, resulting in the generation of additional CO_3^{2-}. The excessive CO_3^{2-} reacted with Ca^{2+} in the solution to produce more $CaCO_3$, thus lowing the overall Mg^{2+}/Ca^{2+} ratio.

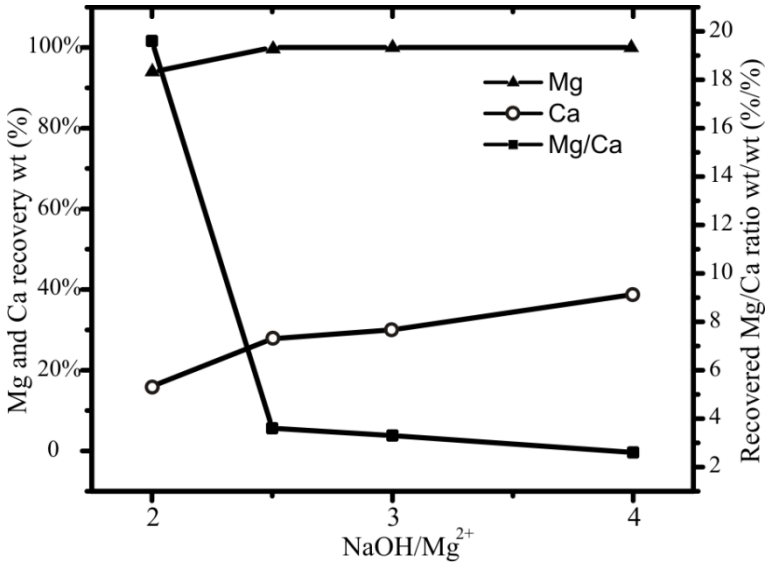

Figure 2 Percentage of Mg^{2+} and Ca^{2+} sequestrated from reject brine as a function of the $NaOH/Mg^{2+}$ molar ratio

3.2 Characterization of the synthesized $Mg(OH)_2$

3.2.1 XRD

Figure 3 shows the XRD diffractograms of $Mg(OH)_2$ obtained from the reaction of reject brine and NaOH at different $NaOH/Mg^{2+}$ molar ratios. The diffraction patterns of all samples demonstrated the presence of $Mg(OH)_2$ along with $CaCO_3$. A shift in the crystal structure of $CaCO_3$ from aragonite to calcite was observed at increased $NaOH/Mg^{2+}$ ratios. This could be attributed to the presence of Mg^{2+} in brine, which inhibited the precipitation of calcite and favored the formation of aragonite at low $NaOH/Mg^{2+}$ ratios [43]. Alternatively, the high pH of the solution at elevated $NaOH/Mg^{2+}$ ratios, at which the influence of Mg^{2+} was minimal, favored the formation of calcite.

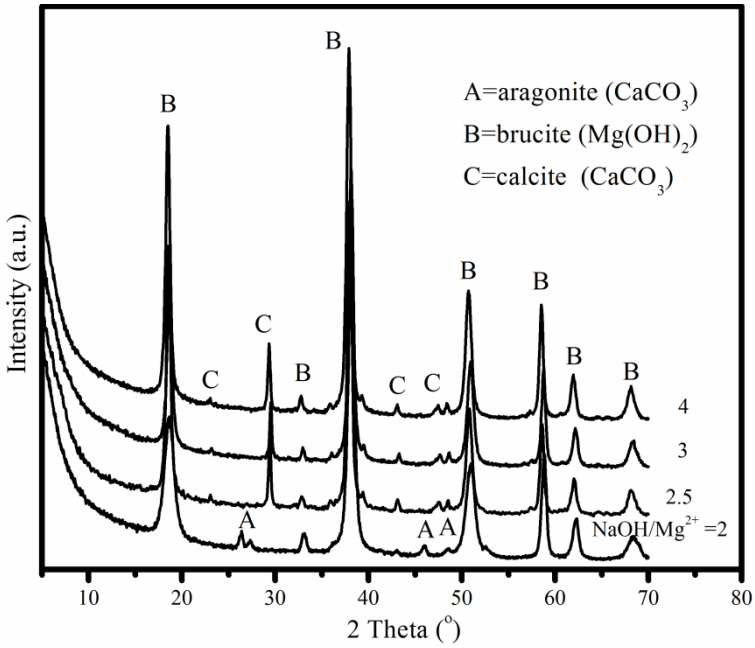

Figure 3 XRD diffractograms of $Mg(OH)_2$ obtained from the reaction of reject brine with NaOH at different $NaOH/Mg^{2+}$ molar ratios

3.2.2 FESEM

The morphologies of $Mg(OH)_2$ samples obtained at different $NaOH/Mg^{2+}$ molar ratios were investigated by FESEM, as shown in Figure 4. A plate-like morphology was observed at a $NaOH/Mg^{2+}$ ratio of 2. The morphology of $Mg(OH)_2$ transformed into a granular pattern consisting of a denser structure at increased $NaOH/Mg^{2+}$ ratios, which could be due to the increased pH of the solution. This was because higher pH values led to the generation of higher concentrations of OH^- in the solution. The increased availability of OH^- accelerated the nucleation of $Mg(OH)_2$ crystals and enabled the formation of larger amounts of $Mg(OH)_2$, facilitating the densification of the overall structure.

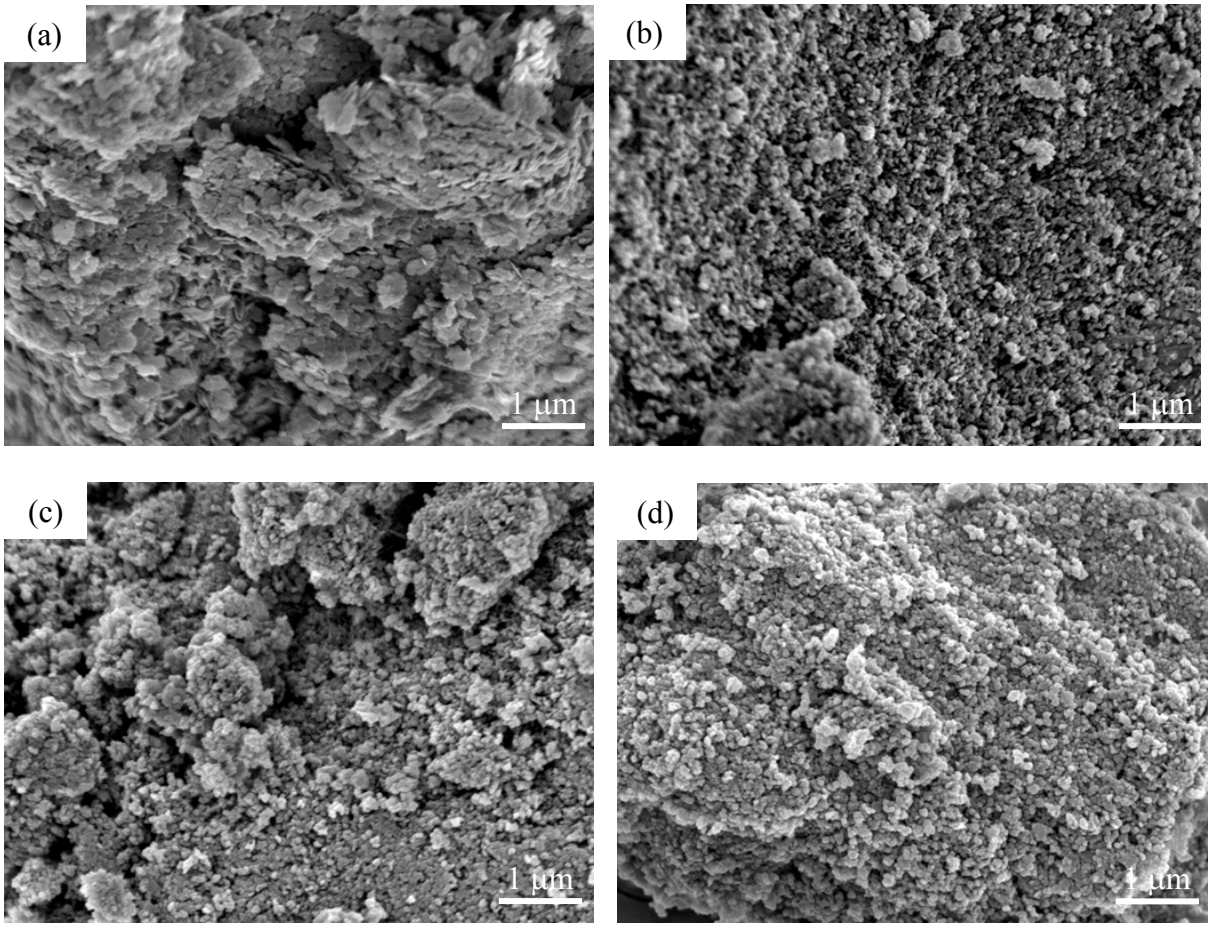

Figure 4 FESEM images of $Mg(OH)_2$ obtained from the reaction of reject brine with NaOH at different NaOH/Mg^{2+} molar ratios of (a) 2, (b) 2.5, (c) 3 and (d) 4

3.2.3 TG/DTA

Figure 5 illustrates a typical TG/DTA graph of $Mg(OH)_2$ obtained via the reaction of brine with NaOH at a NaOH/Mg^{2+} molar ratio of 2. The dehydration of $Mg(OH)_2$ took place at ~400 °C and resulted in a mass loss of around 24.2%, which was attributed to the loss of water. The decomposition patterns observed during TG/DTA were in line with previous studies that investigated the decomposition of $Mg(OH)_2$ into MgO [24, 26-28, 30, 32]. The second endothermic peak, observed at ~720 °C, was due to the decarbonation of $CaCO_3$. The decomposition of $CaCO_3$ led to the release of CO_2, resulting in a mass loss of around 2.3%.

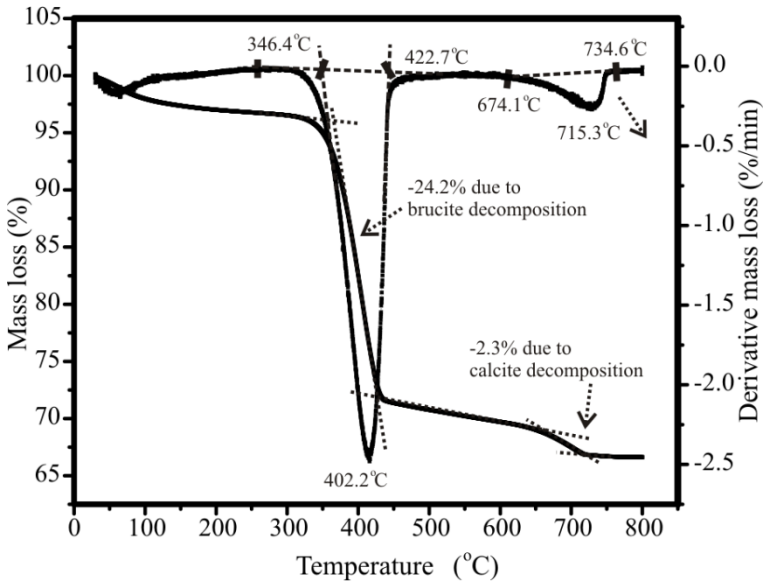

Figure 5 A typical TG/DTA curve of $Mg(OH)_2$ obtained from the reaction of reject brine at a $NaOH/Mg^{2+}$ molar ratio of 2

Table 2 summarizes the TG/DTA results of $Mg(OH)_2$ obtained from the reaction of brine with NaOH at various $NaOH/Mg^{2+}$ ratios ranging between 2 and 4. The results show that the mass loss due to dehydration of $Mg(OH)_2$ at ~400 °C slightly decreased (24.2 to 22.6%), while the mass loss due to decarbonation of $CaCO_3$ at ~720 °C slightly increased (2.3 to 3.9%) with increasing $NaOH/Mg^{2+}$ ratios. This was mainly attributed to the increased content of $CaCO_3$ in the precipitates at higher $NaOH/Mg^{2+}$ ratios, which was in line with the findings shown in Figure 2.

Table 2 TG/DTA results of the decomposition of $Mg(OH)_2$ obtained from the reaction of reject brine with NaOH at different $NaOH/Mg^{2+}$ ratios

Mg^{2+}/ NaOH	Peak temperature (°C)	Mass loss between 340-440 °C (%)	Peak temperature (°C)	Mass loss between 650-750 °C (%)
1:2	402.2	24.2	715.3	2.3
1:2.5	401.2	23.5	721.1	3.2
1:3	400.8	23.3	719.3	3.5
1:4	404.1	22.6	724	3.9

Table 3 compares the compositions of the synthesized $Mg(OH)_2$ based on the TG/DTA (Table 2) and the ICP-OES (Figure 2) results. Both measurements revealed similar trends, showing a decrease in the mass percentage of $Mg(OH)_2$, accompanied with an increase in the mass percentage of $CaCO_3$ (and thus a decrease in the purity of precipitates) with increasing $NaOH/Mg^{2+}$ molar ratios, which was further discussed in Section 3.1. Accordingly, the highest amount of $Mg(OH)_2$ (93.7% by TGA and 95.4% by ICP-OES) was synthesized at a $NaOH/Mg^{2+}$ molar ratio of 2. Therefore, this ratio was chosen as the optimum condition for the subsequent production and characterization of reactive MgO.

Table 3 Composition of synthesized $Mg(OH)_2$ based on TG/DTA and ICP-OES results

Mg^{2+}/NaOH	TG/DTA		ICP-OES	
	$Mg(OH)_2$ (%)	$CaCO_3$ (%)	$Mg(OH)_2$ (%)	$CaCO_3$ (%)
1:2	93.7	6.3	95.4	4.6
1:2.5	91.2	8.8	91.2	8.8
1:3	90.4	9.6	90.6	9.4
1:4	89.2	10.8	88.1	11.9

3.3 Characterization of the synthesized reactive MgO

3.3.1 SSA

Figure 6 presents the SSA of the reactive MgO obtained under different calcination conditions. In general, SSA reduced with increasing calcination temperature and duration, which was in line with the findings of previous studies [24, 26-28, 30, 32]. This was associated with the sintering and agglomeration of MgO grains at higher temperature and prolonged residence times. In the current study, the highest SSA of 51.4 m^2/g was obtained when the synthesized $Mg(OH)_2$ was calcined at 500 ^oC for 2 hours. When compared to other studies, the SSA value (51.4 m^2/g) obtained under these conditions was significantly higher than the results presented in the literature, where MgO synthesized from a magnesium

chloride solution via the addition of NaOH and calcined under the same conditions (i.e. 500 °C for 2 hours), was reported to possess a SSA of 22.1 m^2/g [44]. However, compared with our previous study, MgO calcined at 500 °C for 2 hours from reject brine via the addition of NH_4OH showed a higher SSA of 78.8 m^2/g [31]. This could be because the use of NaOH as the alkali source was found to form $Mg(OH)_2$ with a globular cauliflower-like morphology; while the use of NH_4OH resulted in a more porous plate-like morphology [31]. A relative more porous mother precursor would result in a more porous MgO, thus a higher reactivity. These values can be optimized even further with an adjustment of the calcination temperature and duration towards the lower range, while enabling the complete decomposition of $Mg(OH)_2$.

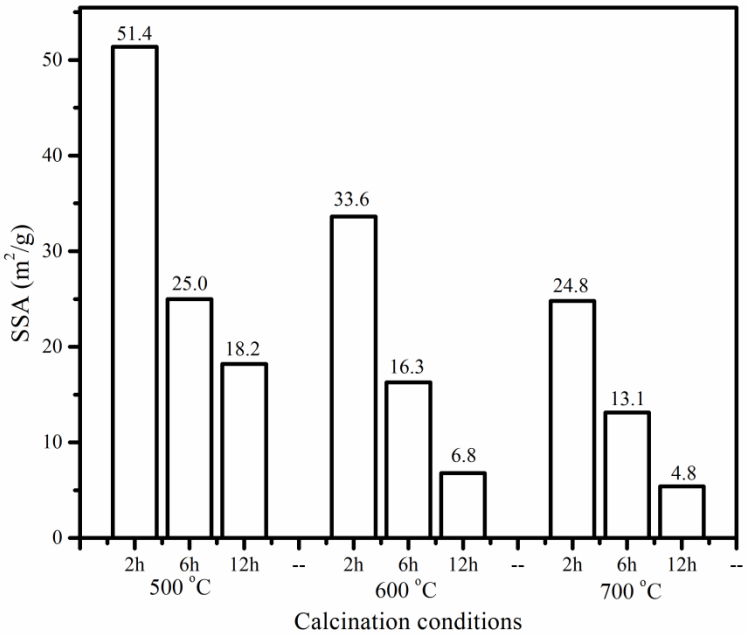

Figure 6 SSA of MgO produced under different calcination temperatures and durations

3.3.2 Reactivity

Figure 7 shows the acid reactivity of MgO obtained under different calcination conditions. An increase in the neutralization time was observed with increasing calcination temperature

and duration, which reflected the reduction in the reactivity of MgO. This observation corresponded well with the SSA measurements reported earlier in Figure 6. A comparison of the reactivity and SSA of MgO is shown in Figure 8, where the inverse correlation between the two parameters was revealed. Accordingly, MgO samples with higher SSA resulted in shorter acid neutralization times, which was an indication of their higher reactivities. These findings were in line with those reported in earlier studies [12, 30], where a direct correlation between the SSA and reactivity of MgO was reported.

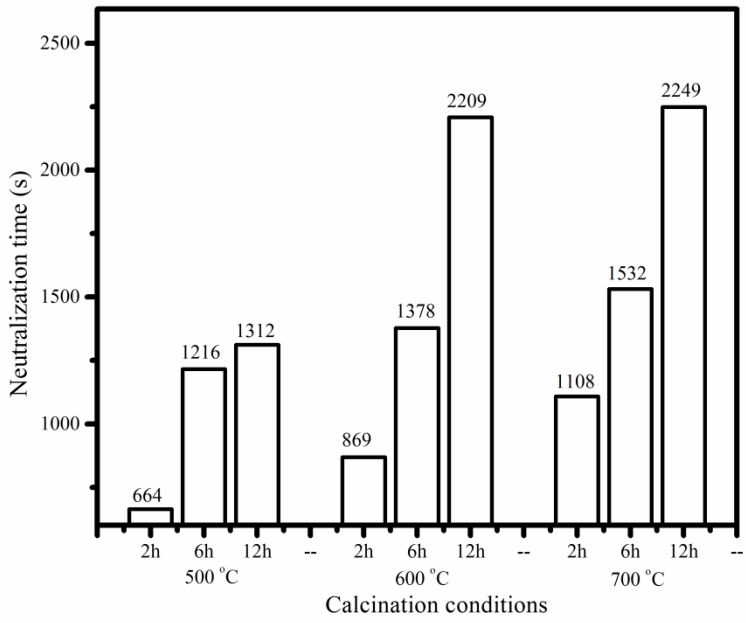

Figure 7 Effect of calcination temperature and duration on the reactivity of MgO

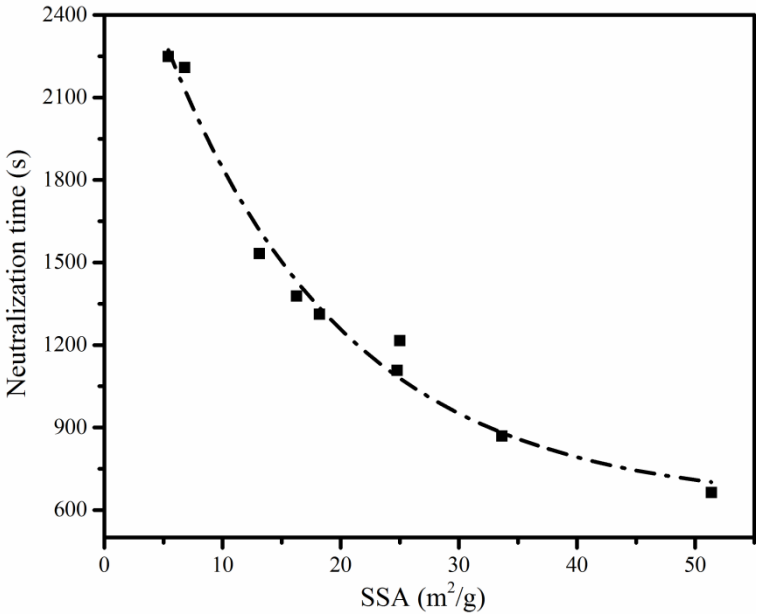

Figure 8 Relationship between the SSA and the reactivity of MgO

3.3.3 XRD

Figure 9 illustrates the diffractograms of MgO obtained via the calcination of $Mg(OH)_2$, which was synthesized at a $NaOH/Mg^{2+}$ molar ratio of 2. The main peak positions of the synthesized MgO were located at ~37.0°, 42.9° and 62.3° 2θ, which matched well with the reference peaks of MgO indicated in JCPDS card no. 89-7746. These peaks were accompanied with a few minor peaks attributed to $CaCO_3$. The absence of $Mg(OH)_2$ peaks indicated the complete decomposition of brucite under the calcination conditions adopted in this study. Aragonite, which was initially present along with $Mg(OH)_2$, transformed into calcite at higher calcination temperatures of 600 °C [45]. A further increase in the calcination temperature (700 °C) and duration led to a reduction in the intensity of the calcite peaks due to decomposition of $CaCO_3$.

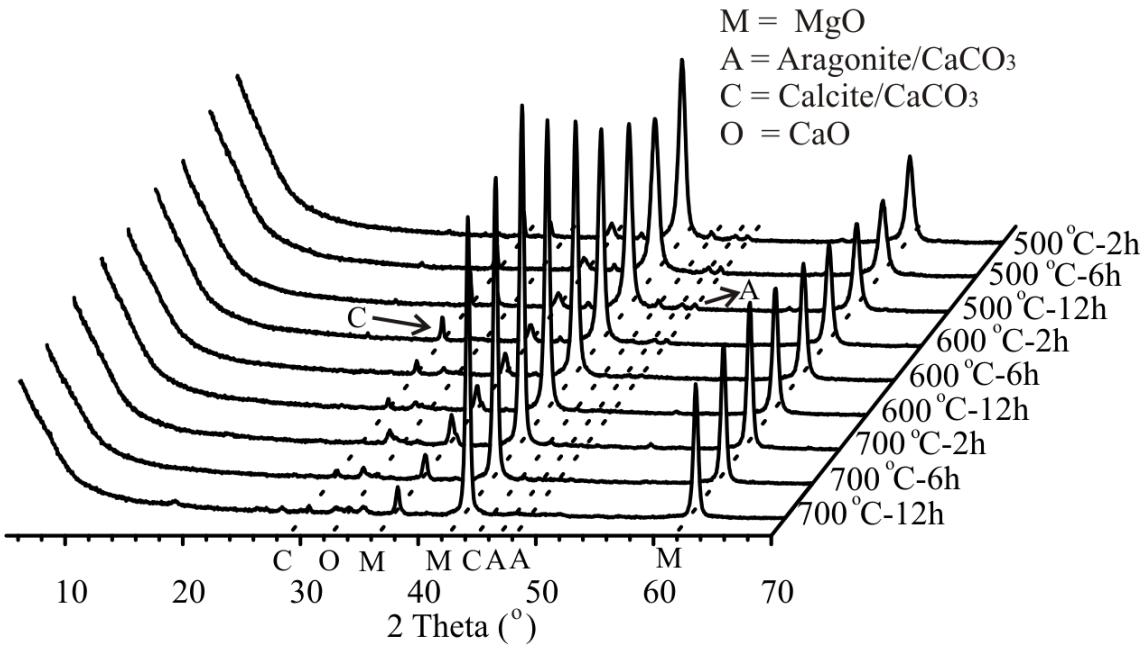

Figure 9 XRD diffractograms of reactive MgO produced via the calcination of $Mg(OH)_2$ under different temperatures and durations

3.3.4 FESEM

A further investigation on the influence of calcination temperature and duration on the SSA of MgO was revealed through FESEM. The changes in the microstructure of MgO at increased temperatures and durations are indicated in Figure 10, which is a good indication of the typical morphology of MgO produced at a calcination temperature of 500-700 °C and a residence time of 2-12 hours. The microstructure of MgO was composed of a single particle which was a combination of several grains. A plate-like morphology, which was inherited from the parent material ($Mg(OH)_2$), was observed throughout the microstructure of MgO produced at lower temperatures. An increase in the particle size, accompanied with the creation of a more porous structure, was observed at increased temperatures and durations. The loss of water during the decomposition of $Mg(OH)_2$ led to the formation of a porous structure, which gradually reduced with the increase in the size of the MgO grains due to continued sintering, causing a reduction in the total pore volume.

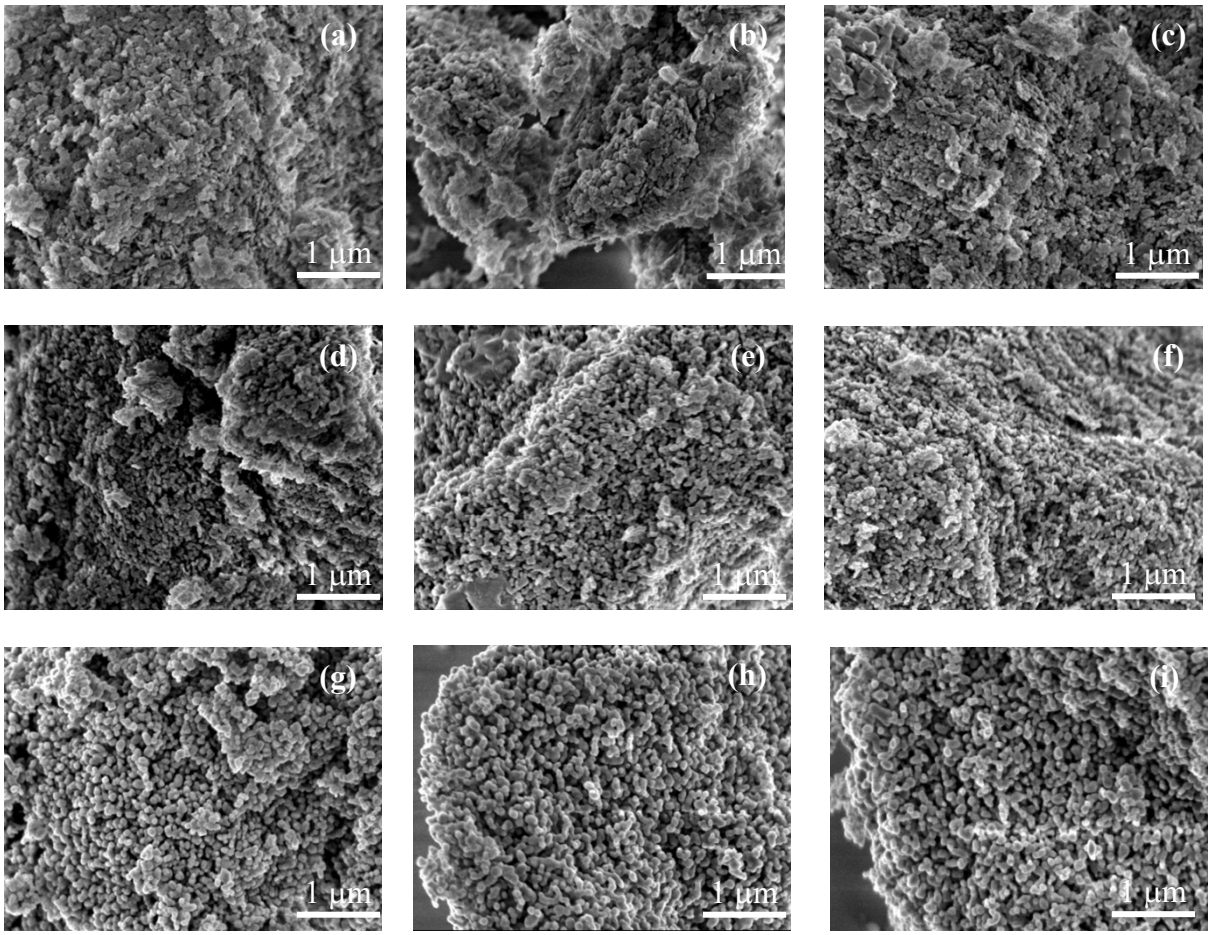

Figure 10 FESEM images of MgO obtained from the calcination of $Mg(OH)_2$ under different conditions: (a) 500°C-2h, (b) 500°C-6h, (c) 500°C-12h, (d) 600°C-2h, (e) 600°C-6h, (f) 600°C-12h, (g) 700°C-2h, (h) 700°C-6h and (i) 700°C-12h

3.4 Economic feasibility

The costs of the production of reactive MgO from reject brine via the addition of NaOH, NH_3, or CaO were calculated and compared. In the first step, base is added into reject brine to precipitate $Mg(OH)_2$. Raw material costs of NaOH, NH_3, and CaO are reported to be ~S$571/ton NaOH [46], ~S$525/ton NH_3 [47], and ~S$170/ton CaO [48], respectively. Cost of reject brine, transportation of raw materials, and grinding and packing of reactive MgO are not considered. Since a production yield of 1 ton reactive MgO requires 2 tons NaOH, 1 ton

373 NH_3, or 1.4 ton CaO as the base source, the raw material costs are calculated to be
374 S$1142/ton MgO, S$525/ton MgO and S$238/ton MgO via the addition of NaOH, NH_3, or
375 CaO, respectively.
376
377 The resulting $Mg(OH)_2$ produced in the first step was in the form of filter cake which consists
378 of 55.2% solids and 44.8% free water. In the second step, $Mg(OH)_2$ filter cake was calcinated
379 to produce MgO. Energy consumption during calcination of $Mg(OH)_2$ filter cake is derived
380 by considering the following two steps: (i) Energy consumed to increase the temperature
381 from room temperature (298 K, 25 °C) to the decomposition temperature of $Mg(OH)_2$ (773K,
382 500 °C), and (ii) enthalpy of decomposition of $Mg(OH)_2$ [3]. A production yield of 1 ton
383 MgO requires decomposing 1.45 ton $Mg(OH)_2$ and the decomposition temperature of
384 $Mg(OH)_2$ under one atmosphere CO_2 pressure is in the range between 773 and 973 K (500
385 and 700 °C). Firstly the energy required to raise the temperature from ambient air (298 K) to
386 the decomposition temperature (773 K) is calculated using the formula: C_p × increase in
387 temperature (K). The specific heat capacity (C_p) of $Mg(OH)_2$ at 773 K is 1.78 kJ/kg K, which
388 results in the energy demand of 1.15 GJ in consideration of the purity of the synthesized
389 $Mg(OH)_2$ of ~94%. The energy required for decomposition of $Mg(OH)_2$ is calculated based
390 on the enthalpy of decomposition (1304 kJ/kg K), which brings in 1.77 GJ. As for the free
391 water, energy required to increase temperature of free water from room temperature (298 K)
392 to the boiling point (373 K) is calculated based on the specific heat capacity of water (4.18
393 kJ/kg K) and the percentage of water in the filter cake (44.8%), resulting in 0.37 GJ. This is
394 followed by the enthalpy of the vaporization of water (2283 kJ/kg K), resulting in 2.69 GJ.
395 Finally the energy required to heat up the resultant steam to 773 K is calculated via the heat
396 capacity of water vapour (1.86 kJ/kg K), bringing in 0.88 GJ. The total energy required for
397 the calcination process is the summation of the energy required for each individual step,

resulting in a total of 6.85 GJ (1902.8 kWh) for the production of 1 ton reactive MgO from reject brine via the addition of base. As of 2015, Singapore uses natural gas (95%) and others (4%) for the power generation at a price of 20.2 cents per kWh [49], which results in an energy cost of S$384 to product 1 ton reactive MgO from reject brine via the addition of a base.

Production cost of the resulting MgO via the addition of NaOH, NH_3, and CaO in reject brine are S$1526, S$909, and S$622 per ton MgO, respectively, as shown in Figure 11. Price of MgO produced via a dry route in the US market was reported to be S$617 per ton MgO [50]. Thus, a cheaper base alternative would make the production of reactive MgO from reject brine more economically feasible. Furthermore, synthetic MgO from reject brine shows a much higher purity and reactivity compared to the dry route as the SSA of commercial MgO is usually ~20 m^2/g [3], which makes synthetic MgO more competitive in the global market.

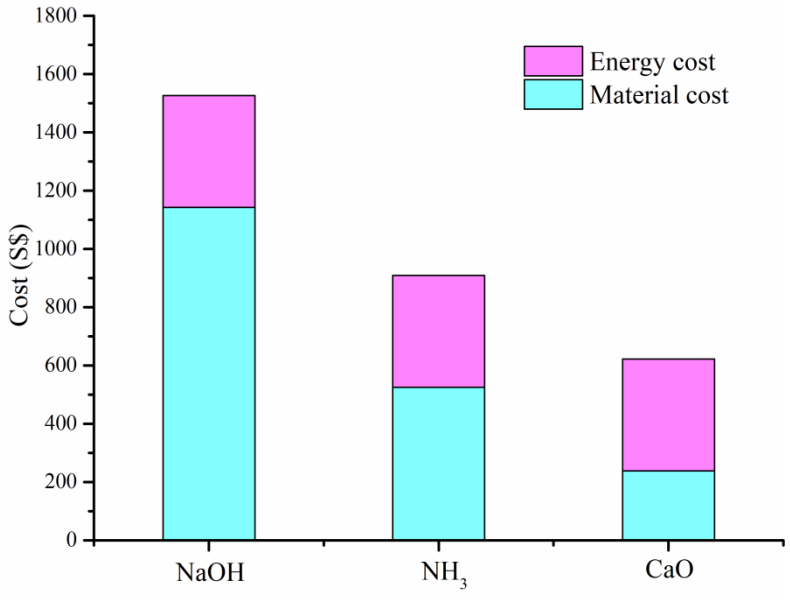

Figure 11 Production cost of reactive MgO from reject brine via the addition of NaOH, NH_3, or CaO.

4 Conclusions

This study presented a comprehensive investigation on the synthesis of $Mg(OH)_2$ and production of reactive MgO from reject brine via the use of NaOH. The key parameters affecting the properties of the synthesized $Mg(OH)_2$ and its calcination to produce reactive MgO were revealed. The results demonstrated the feasibility of recovering reactive MgO from reject brine obtained as a waste at the end of the desalination process. The initial set of experiments successfully demonstrated the use of NaOH as an alkali source in the precipitation of $Mg(OH)_2$ from reject brine. The effect of the $NaOH/Mg^{2+}$ ratio on the final yield was investigated with the goal of optimizing the amount and purity of the synthesized $Mg(OH)_2$. An optimum $NaOH/Mg^{2+}$ ratio of 2, which generated the highest purity of $Mg(OH)_2$, was determined and used in the subsequent production of MgO. The influence of calcination conditions (i.e. temperature and residence time) on the reactivity of MgO obtained via the calcination of the synthesized $Mg(OH)_2$ were reported. While a certain minimum temperature was required for the complete decomposition of $Mg(OH)_2$ into MgO, an increase in the calcination temperature and duration lowered the reactivity of MgO. Calcination of $Mg(OH)_2$ at 500 ºC for 2 hours resulted in the most reactive MgO samples, with a SSA of 51.4 m^2/g. This study demonstrated that reject brine can be considered as a feasible and economic alternative source for the sustainable recovery of MgO with a high reactivity, which can be used in various applications within the food, cosmetics, pharmaceutical and construction industries [1-3].

Acknowledgement

This project is funded by the National Research Foundation (NRF), Prime Minister's Office, Singapore under its Campus for Research Excellence and Technological Enterprise (CREATE) program. Special thanks to Ms. Rui Hao for her review and comments of the

441 manuscript.

442

444 **References**

445 [1] D.A. Kramer, Magnesium, its alloys and compounds, Industrial Minerals and Rocks,
446 2001.

447 [2] E.K. Lee, K.D. Jung, O.S. Joo, Y.G. Shul, Magnesium oxide as an effective catalyst in
448 catalytic wet oxidation of H2S to sulfur, Reaction Kinetics and Catalysis Letters, 82, 2004,
449 241-246.

450 [3] M.A. Shand, The chemistry and technology of magnesia, 2006.

451 [4] M.A. Caraballo, T.S. Rotting, F. Macias, J.M. Nieto, C. Ayora, Field multi-step limestone
452 and MgO passive system to treat acid mine drainage with high metal concentrations, Applied
453 Geochemistry, 24, 2009, 2301-2311.

454 [5] L.W. Mo, M. Deng, M.S. Tang, A. Al-Tabbaa, MgO expansive cement and concrete in
455 China: Past, present and future, Cement and Concrete Research, 57, 2014, 1-12.

456 [6] A.J.W. Harrison, Reactive magnesium oxide cements, 2008.

457 [7] M. Liska, A. Al-Tabbaa, K. Carter, J. Fifield, Scaled-up commercial production of
458 reactive magnesium cement pressed masonry units. Part I: Production, Proceedings of the
459 Institution of Civil Engineers-Construction Materials, 165, 2012a, 211-223.

460 [8] M. Liska, A. Al-Tabbaa, K. Carter, J. Fifield, Scaled-up commercial production of
461 reactive magnesia cement pressed masonry units. Part II: Performance, Proceedings of the
462 Institution of Civil Engineers-Construction Materials, 165, 2012b, 225-243.

463 [9] C. Unluer, A. Al-Tabbaa, Impact of hydrated magnesium carbonate additives on the
464 carbonation of reactive MgO cements, Cement and Concrete Research, 54, 2013, 87-97.

465 [10] C. Unluer, A. Al-Tabbaa, Enhancing the carbonation of MgO cement porous blocks
466 through improved curing conditions, Cement and Concrete Research, 59, 2014, 55-65.

467 [11] A. Al-Tabbaa, Reactive magnesia cement, in: F. PachecoTorgal, S. Jalali, J. Labrincha,
468 V.M. John (Eds.) Eco-Efficient Concrete, 2013, pp. 523-543.

469 [12] F. Jin, A. Al-Tabbaa, Characterisation of different commercial reactive magnesia,
470 Advances in Cement Research, 26, 2014, 101-113.
471 [13] Y. Soong, A.L. Goodman, J.R. McCarthy-Jones, J.P. Baltrus, Experimental and
472 simulation studies on mineral trapping of CO2 with brine, Energy Conversion and
473 Management, 45, 2004, 1845-1859.
474 [14] M.L. Druckenmiller, M.M. Maroto-Valer, Carbon sequestration using brine of adjusted
475 pH to form mineral carbonates, Fuel Processing Technology, 86, 2005, 1599-1614.
476 [15] R. Hao, Investigation into the Production of Carbonates and Oxides from Synthetic
477 Brine through Carbon Sequestration, in: Department of Engineering, University of
478 Cambridge, 2017.
479 [16] R. Friedrich, H. Robinson, R. Spencer, Magnesium hydroxide from sea water, in,
480 Google Patents, 1946.
481 [17] N. Petric, V. Martinac, M. Labor, The effect of mannitol and pH of the solution on the
482 properties of sintered magnesium oxide obtained from sea water, Chemical Engineering &
483 Technology, 20, 1997, 36-39.
484 [18] M. Turek, W. Gnot, Precipitation of magnesium hydroxide from brine, Industrial &
485 Engineering Chemistry Research, 34, 1995, 244-250.
486 [19] R.H. Dave, P.K. Ghosh, Enrichment of bromine in sea-bittern with recovery of other
487 marine chemicals, Industrial & Engineering Chemistry Research, 44, 2005, 2903-2907.
488 [20] M.H. El-Naas, Reject brine management, in: Desalination, trends and technologies,
489 InTech, 2011, pp. 237-252.
490 [21] K.T. Tran, T. Van Luong, J.W. An, D.J. Kang, M.J. Kim, T. Tran, Recovery of
491 magnesium from Uyuni salar brine as high purity magnesium oxalate, Hydrometallurgy, 138,
492 2013, 93-99.

493 [22] T. Khuyen Thi, K.S. Han, S.J. Kim, M.J. Kim, T. Tam, Recovery of magnesium from
494 Uyuni salar brine as hydrated magnesium carbonate, Hydrometallurgy, 160, 2016, 106-114.
495 [23] S. Casas, C. Aladjem, E. Larrotcha, O. Gibert, C. Valderrama, J.L. Cortina, Valorisation
496 of Ca and Mg by-products from mining and seawater desalination brines for water treatment
497 applications, Journal of Chemical Technology and Biotechnology, 89, 2014, 872-883.
498 [24] W.R. Eubank, Calcination studies of magnesium oxides, Journal of the American
499 Ceramic Society, 34, 1951, 225-229.
500 [25] J. Green, Calcination of precipitated Mg (OH) 2 to active MgO in the production of
501 refractory and chemical grade MgO, Journal of Materials Science, 18, 1983, 637-651.
502 [26] K. Itatani, K. Koizumi, F.S. Howell, A. Kishioka, M. Kinoshita, Agglomeration of
503 magnesium oxide particles formed by the decomposition of magnesium hydroxide .1.
504 Agglomeration at increasing temperature, Journal of Materials Science, 23, 1988, 3405-3412.
505 [27] V. Choudhary, V. Rane, R. Gadre, Influence of precursors used in preparation of MgO
506 on its surface properties and catalytic activity in oxidative coupling of methane, Journal of
507 Catalysis, 145, 1994, 300-311.
508 [28] E. Alvarado, L.M. Torres-Martinez, A.F. Fuentes, P. Quintana, Preparation and
509 characterization of MgO powders obtained from different magnesium salts and the mineral
510 dolomite, Polyhedron, 19, 2000, 2345-2351.
511 [29] I.F. Mironyuk, V.M. Gun'ko, M.O. Povazhnyak, V.I. Zarko, V.M. Chelyadin, R.
512 Leboda, J. Skubiszewska-Zięba, W. Janusz, Magnesia formed on calcination of Mg(OH)2
513 prepared from natural bischofite, Applied Surface Science, 252, 2006, 4071-4082.
514 [30] L.W. Mo, M. Deng, M.S. Tang, Effects of calcination condition on expansion property
515 of MgO-type expansive agent used in cement-based materials, Cement and Concrete
516 Research, 40, 2010, 437-446.

517 [31] H. Dong, C. Unluer, E.-H. Yang, A. Al-Tabbaa, Synthesis of reactive MgO from reject
518 brine via the addition of NH_4OH, Hydrometallurgy, 169, 2017, 165-172.
519 [32] J.K. Bartley, C. Xu, R. Lloyd, D.I. Enache, D.W. Knight, G.J. Hutchings, Simple
520 method to synthesize high surface area magnesium oxide and its use as a heterogeneous base
521 catalyst, Applied Catalysis B: Environmental, 128, 2012, 31-38.
522 [33] L.F. Greenlee, D.F. Lawler, B.D. Freeman, B. Marrot, P. Moulin, Reverse osmosis
523 desalination: water sources, technology, and today's challenges, Water research, 43, 2009,
524 2317-2348.
525 [34] C. Fritzmann, J. Lowenberg, T. Wintgens, T. Melin, State-of-the-art of reverse osmosis
526 desalination, Desalination, 216, 2007, 1-76.
527 [35] ST, Fifth Singapore desalination plant in the pipeline, in, The Straits Times, The Straits
528 Times, 2016.
529 [36] IDA, The current state of desalination, in, International Desalination Association, 2015.
530 [37] S. Adham, A. Hussain, J.M. Matar, R. Dores, A. Janson, Application of Membrane
531 Distillation for desalting brines from thermal desalination plants, Desalination, 314, 2013,
532 101-108.
533 [38] A.M.O. Mohamed, M. Maraqa, J. Al Handhaly, Impact of land disposal of reject brine
534 from desalination plants on soil and groundwater, Desalination, 182, 2005, 411-433.
535 [39] M.H. El-Naas, A.H. Al-Marzouqi, O. Chaalal, A combined approach for the
536 management of desalination reject brine and capture of CO2, Desalination, 251, 2010, 70-74.
537 [40] D.H. Kim, A review of desalting process techniques and economic analysis of the
538 recovery of salts from retentates, Desalination, 270, 2011, 1-8.
539 [41] M. Elimelech, W.A. Phillip, The Future of Seawater Desalination: Energy, Technology,
540 and the Environment, Science, 333, 2011, 712-717.

[42] L.G. Sillen, A.E. Martell, J. Bjerrum, Stability constants of metal-ion complexes, Chemical Society London, 1964.

[43] R.A. Berner, The role of magnesium in the crystal growth of calcite and aragonite from sea water, Geochimica et Cosmochimica Acta, 39, 1975, 489-504.

[44] T.G. Venkatesha, R. Viswanatha, Y.A. Nayaka, B.K. Chethana, Kinetics and thermodynamics of reactive and vat dyes adsorption on MgO nanoparticles, Chemical Engineering Journal, 198, 2012, 1-10.

[45] C.G. Kontoyannis, N.V. Vagenas, Calcium carbonate phase analysis using XRD and FT-Raman spectroscopy, The Analyst, 125, 2000, 251-255.

[46] Y. Fukushima, Caustic soda prices on upward trend in Asian markets, 2016.

[47] A. Jones, Why do ammonia prices keep falling?, 2016.

[48] USGS, Minerals yearbook-lime 2012, 2012.

[49] EMA, Singapore energy statistics 2016, Energy Market Authority, 2016.

[50] S. Bogner, MGX minerals plans to enter the magnesium market in 2016, Rockstone Reserach Ltd., 2015.

Highlights

- Recovery of reactive MgO from reject brine via addition of NaOH
- An optimum NaOH/Mg^{2+} ratio of 2 leads to the highest purity of $Mg(OH)_2$
- Resulting MgO with a SSA of 51.4 m^2/g
- Reject brine can be an economic alternative source for recovery of highly reactive MgO

Recovery of reactive MgO from reject brine via the addition of NaOH

Haoliang Dong[a], Cise Unluer[a], En-Hua Yang[a,*], Abir Al-Tabbaa[b]

[a] School of Civil and Environmental Engineering, Nanyang Technological University, 50 Nanyang Avenue, Singapore 639798, Singapore

[b] Department of Engineering, University of Cambridge, Trumpington Street, Cambridge CB2 1PZ, UK

Abstract

Reject brine, generated as a waste at the end of the desalination process, presents a useful source for the extraction of valuable resources. This study investigated the recovery of reactive MgO from reject brine obtained from a local desalination plant. This was enabled via the reaction of Mg^{2+} present within reject brine with an alkali source (NaOH), which led to the precipitation of $Mg(OH)_2$, along with a small amount of $CaCO_3$. The determination of the optimum $NaOH/Mg^{2+}$ ratio led to the production of the highest amount of yield. The synthesized $Mg(OH)_2$ was further calcined under a range of temperatures (500-700 °C) and durations (2-12 hours) to produce reactive MgO. A detailed characterization of MgO obtained under these conditions was presented in terms of its reactivity, specific surface area (SSA), composition and microstructure. While an increase in the calcination temperature and duration decreased the reactivity and SSA of MgO, samples calcined at 500 °C for 2 hours revealed the highest reactivity, which was reflected by their SSA of 51.4 m^2/g.

Keywords: Reject brine; reactive MgO; NaOH; $Mg(OH)_2$; calcination

* Corresponding author. Address: N1-01b-56, 50 Nanyang Avenue, Singapore 639798. Tel.: +65 6790 5291; fax: +65 6791 0676. *E-mail:* ehyang@ntu.edu.sg

1 Introduction

Magnesium oxide (MgO) finds use in various applications ranging from the refractory industry to agriculture, chemical and environmental applications [1-4]. Another increasingly popular use of reactive MgO was reported in the construction industry as an expansive additive [5] and as a novel binder in the development of concrete formulations [6-11]. While the majority of MgO produced today is obtained through the processing of naturally occurring minerals such as magnesite ($MgCO_3$) [3], around 14% of the global MgO supply is from the calcination of magnesium hydroxide ($Mg(OH)_2$) synthesized from seawater or magnesium-rich brine sources. The synthetic MgO obtained from seawater/brine demonstrates a higher purity and reactivity compared with MgO produced through the calcination of magnesite [12]. MgO that possesses higher purity and specific surface area (SSA) is widely used in high-end pharmaceutical and semiconductor applications as an additive or a catalyst [1-4].

The recovery of brucite ($Mg(OH)_2$) from seawater/brine deploys the use of a strong base to precipitate Mg^{2+} from the solution. During this process, it is essential to reach an appropriate pH level in order to form the precipitates. Previous studies [13, 14] have shown that the ideal pH for the formation of carbonates is above 9, which favors the transformation of carbon dioxide and bicarbonates to CO_3^{2-}. The pH level of gelatinous $Mg(OH)_2$ could be even higher due to the requirement of surplus hydroxide. These trends were also confirmed by [15], who demonstrated the occurrence of the precipitation process at a pH of 8.5, whereas higher pH values led to increased brucite formation.

Lime (CaO) [16] or dolomite lime (CaO·MgO) [17] are used as a base during the synthesis of $Mg(OH)_2$ from seawater. The use of dolomite lime reduces the amount of seawater/brine

needed for the production of the same amount of MgO obtained via the use of CaO because dolomite lime itself contains MgO. However, the uses of these Ca-bearing bases often lead to the precipitation of Ca-based compounds (e.g. $CaCO_3$) and thus reduce the purity and content of Mg-based precipitates. Furthermore, the Ca-bearing bases can react with sulphate (SO_4^{2-}) present in the solution to form gypsum ($CaSO_4 \cdot 2H_2O$), which may necessitate the pre-treatment of the solution through the addition of $CaCl_2$ to remove sulphate in seawater/brine.

Apart from Ca-based bases, several studies have suggested the use of other alkali sources to precipitate Mg^{2+} from seawater/brine [15, 18-23]. $NaCO_3$ and NaOH were reported to recover Ca and Mg from mining and seawater desalination brines. Recovery ratios higher than 94-96 % of Ca were achieved for pH higher than 10 via the use of $NaCO_3$ and recovery ratios higher than 97-99 % of Mg were achieved for pH higher than 11 via the addition of NaOH [23]. Another proposed additives was sodium hydroxide (NaOH) along with oxalic acid, which produce magnesium oxalate (MgC_2O_4) from brine. Previous studies [21] demonstrated the selective precipitation of Mg- and Ca-oxalate at different pH values. Ca-oxalate was first precipitated and removed at an oxalate/Ca molar ratio of 6.82 at a pH of < 1. This was followed by the precipitation of Mg^{2+} from the brine residue at a NaOH/oxalate/Mg ratio of 3.21:1:1.62 at a pH range of 3-5.5, leading to a high yield of pure magnesium oxalate.

These steps can be followed by the production of reactive MgO via the calcination of Mg-containing precipitates, such as magnesium hydroxide and magnesium oxalate. Numerous studies have been carried out to characterize MgO obtained from different sources [12, 24-32]. The outcomes of these studies have identified the main factors that influence the properties of MgO produced through the dry route (i.e. decomposition of magnesite) as the calcination conditions (i.e. temperature and residence time). Accordingly, increased

calcination temperatures and/or prolonged durations lead to the agglomeration of MgO particles due to sintering, which decreases the porosity and reactivity of MgO [30].

Desalination provides an alternative means to meet the residential and industrial water demands in water-stressed countries like Singapore [33, 34]. Currently, the two desalination plants in Singapore provide 100 million gallons (448,500 m^3) of drinking water on a daily basis, which can meet 25% of Singapore's current water demand. With three additional desalination plants being built, the five desalination plants are designed to provide a total of 190 million gallons (852,150 m^3) of water per day by 2020 [35]. On a global level, the daily production level of desalinated water by 18,426 desalination plants exceeds 86.8 million cubic meters [36]. Production of desalinated water generates an almost equal amount of reject brine [20], a high salt concentration waste by-product produced at the end of the desalination process [37]. Reject brine is often discharged directly back into sea, which threatens the marine life and ecosystem by altering the local flora and fauna due to its high salinity [38]. Therefore, the disposal and management of reject brine remains a major challenge as well as an environmental threat [38, 39], which can pave the way for its use in the recovery of valuable metals and useful solids instead of direct discharge [40].

The desalination process involves the addition of a variety of chemicals to enable the precipitation of the colloidal particles before running through the filtration process. Therefore, the resulting reject brine contains a very high concentration of dissolved salts and suspended constituents, creating variations in its composition in comparison to seawater, natural brine or synthetic solutions. While previous studies [15, 18-22] have reported the synthesis of MgO or its derivatives from seawater, natural brine or synthetic solutions, this study aims to explore the feasibility of the recovery of Mg^{2+} from reject brine collected from

a local desalination plant. The proposed method involves the addition of NaOH, which serves as a pH adjuster and controls the pH of the solution. Unlike Ca-bearing bases, which often lead to the precipitation of a Ca-based compound (e.g. $CaCO_3$) along with Mg-phases, the use of NaOH can increase the purity of Mg-based precipitates. Furthermore, when compared with other bases (e.g. NH_4OH, KOH and Na_2CO_3), NaOH possesses other advantages in terms of health and safety, cost effectiveness and base strength it provides [31].

This research presents a comprehensive study on the synthesis of $Mg(OH)_2$ and production of reactive MgO from reject brine via the use of NaOH. The key parameters affecting the properties of the synthesized $Mg(OH)_2$ and its calcination to produce reactive MgO were investigated. Several techniques were utilized to characterize the synthesized $Mg(OH)_2$ and MgO including inductively coupled plasma-optical emission spectroscopy (ICP-OES), X-ray powder diffraction (XRD), field emission scanning electron microscopy (FESEM), thermogravimetric and differential thermal analysis (TG/DTA), Brunauer-Emmett-Teller (BET) analysis and acid neutralization. Production cost of reactive MgO from reject brine via the addition of NaOH was calculated to evaluate the economic feasibility of the approach. Results obtained at the end of this study were used to demonstrate the use of reject brine as an alternative source for the recovery of MgO with a high reactivity.

2 Materials and Methodology

2.1 Materials

Reject brine was collected and sampled from a local desalination plant in Singapore, which adopts a reverse osmosis (RO) membrane system to purify saline water and produce drinkable water for human use. These membranes reject more than 99.5% of the dissolved

salts and suspended materials in the feedwater, resulting in a highly concentrated reject waste stream which contains suspended constituents and a 2- to 7-fold increased concentration of dissolved salts [33, 34, 41]. Prior to any analysis, the reject brine was first filtrated through a 45 μm membrane filter to remove the large suspended solids. The pH of reject brine as received was around 8.0. The chemical composition of the reject brine, obtained via inductively coupled plasma-optical emission spectroscopy (ICP-OES) and ion chromatography (IC), is summarized in Table 1. Along with Mg^{2+}, which was present at a concentration of 1718 ppm, other impurities such as Na^{+}, K^{+} and Ca^{2+} were also identified in the reject brine. Sodium hydroxide (NaOH, reagent grade, pellets) supplied by VWR Pte Ltd in Singapore, was used as the alkaline base in the current study.

Table 1 Chemical composition of the reject brine used in this study

Element	Cl	Na	SO_4	Mg	K	Ca	Sr	B	Si	Li	P	Al
Concentration (ppm)	55243	13580	4423	1718	845.7	471.3	14.6	3.8	3.7	0.3	0.2	0.1

2.2 Methodology

Different amounts of NaOH solution (16 M) were added into 200 ml of reject brine to study the influence of $NaOH/Mg^{2+}$ molar ratio (ranging from 2 to 4) on the recovery of Mg^{2+}. NaOH solution was added into reject brine at once and the initial pH of solution was recorded. The solution was mixed at constant speed of 300 rpm by a magnetic stirrer at room temperature (25 °C). A pH/thermometer probe was used to monitor and record the temperature and pH of the reaction in the solution. Experiment was terminated when the pH of the solution stabilized. The solids were separated from the residual brine through a centrifuge. After the solids were collected, they were re-dispersed and washed thoroughly by ultra-pure water in an ultrasonic bath to remove surface-attached ions. The washed solids were separated from the solution through a centrifuge. This washing process was repeated for

three times to remove surface-attached ions and soluble salts. The washed solids were then oven-dried at 105 °C for 24 hours to remove free water before grinding into powder form. The ground samples were calcined at pre-determined temperatures (500-700 °C) and durations (2-12 hours) in an electric furnace to produce reactive MgO.

Several techniques were utilized to characterize the synthesized $Mg(OH)_2$ and MgO. X-ray powder diffraction (XRD) was performed via a Bruker D8 Advance with a Cu Kα source under the operation conditions of 40 kV and 40 mA, emitting radiation with a wavelength of 1.5405 angstroms, scan rate of 0.02 °/step, and a 2θ range of 5 to 70°. A JSM-7600F thermal field emission scanning electron microscopy (FESEM) was used to analyze the microstructure of the solids by imaging powder surface. The decomposition of each sample was studied via thermogravimetric and differential thermal analysis (TG/DTA) using a PyrisDiamond TGA 4000 operated at a heating rate of 10 °C/min under air flow. The specific surface area (SSA) of the synthesized samples was obtained by Brunauer-Emmett-Teller (BET) analysis from nitrogen adsorption-desorption isotherms using a Quadrasorb Evo automated surface area and pore size analyser. The reactivity of MgO was measured by acid neutralization, during which 0.28 grams of the synthesized MgO was added into 50 ml of 0.07 mol/L citric acid solution along with phenolphthalein (i.e. pH indicator). The neutralization time was measured and reported as an indicator of reactivity [3, 30].

Economic feasibility of the production of reactive MgO from reject brine in this study was evaluated and compared with other production routes. The total cost of the production of reactive MgO from reject brine mainly consists of the raw material cost for synthesis (e.g. NaOH) and the energy cost during calcination. Reject brine is the waste water produced at the end in the desalination plant, and thus the material cost and energy cost of reject brine are

assumed to be zero. Transportation of raw materials and the grinding and packing of reactive MgO products are not considered into the calculation since they do not contribute significantly to the overall process.

3 Results and Discussion

3.1 Recovery of Mg^{2+} and Ca^{2+} from reject brine

The formation of $Mg(OH)_2$ was observed via the reaction between the Mg^{2+} in the reject brine and OH^- provided by NaOH. The addition of NaOH also enabled the conversion of HCO_3^-, present in the reject brine, to CO_3^{2-}. This led to a reaction of CO_3^{2-} with Ca^{2+} and resulted in the precipitation of $CaCO_3$. The reaction paths observed during this process are shown in Equations 1-4 below.

$$NaOH_{(aq)} \rightarrow Na^+ + OH^- \quad (1)$$

$$Mg^{2+} + 2OH^- \leftrightarrow Mg(OH)_2 \quad (2)$$

$$NaOH_{(aq)} + HCO_3^- \leftrightarrow CO_3^{2-} + Na^+ + H_2O \quad (3)$$

$$Ca^{2+} + CO_3^{2-} \leftrightarrow CaCO_3 \quad (4)$$

The kinetics of the reaction between reject brine and NaOH reflected by the change of pH are summarized in Figure 1. A rapid reaction was observed, which was completed in less than 30 minutes as the pH reached an equilibrium state. The pH increased with the molar ratio of $NaOH/Mg^{2+}$. This was due to the increased concentration of OH^- provided by the higher amounts of NaOH introduced into the solution, whereas a smaller increase was observed at $NaOH/Mg^{2+}$ ratios of > 2.5.

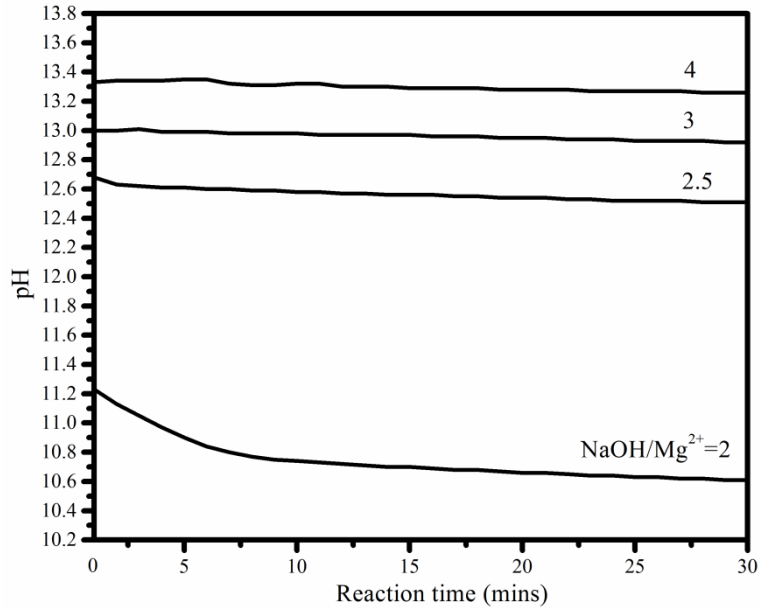

Figure 1 pH of the reaction between reject brine and NaOH at different $NaOH/Mg^{2+}$ ratios

Figure 2 shows the recovery rate of Mg^{2+} and Ca^{2+} in weight percentage after the reaction of reject brine with NaOH. As can be seen, the recovery rates for both Mg^{2+} and Ca^{2+} increased with increasing $NaOH/Mg^{2+}$ molar ratio, which achieved a similar recovery level of 94-99% of Mg as reported in [23]. The recovered Mg^{2+}/Ca^{2+} ratio was used as an indication of the purity level of the resulting $Mg(OH)_2$ precipitates. As shown in Figure 2, Mg^{2+}/Ca^{2+} was highest (19.6) at a $NaOH/Mg^{2+}$ ratio of 2 and decreased with increasing $NaOH/Mg^{2+}$ ratio. This was because at a $NaOH/Mg^{2+}$ molar ratio of 2, the ion product in the solution ($[Mg^{2+}][OH^-]^2 = 7\times10^{-8.6}$ $mol^3\ l^{-3}$, pH = 11.2) was larger than the solubility product constant of $Mg(OH)_2$ (1.8×10^{-11} $mol^3\ l^{-3}$) [42]. The supersaturation condition enabled the reaction between OH^- and Mg^{2+} and the formation of $Mg(OH)_2$. Furthermore, pH increased with increasing $NaOH/Mg^{2+}$, which provided excessive OH^- in the solution to attack HCO_3^-. This caused in a shift in Equation 3 towards the right hand side, resulting in the generation of additional CO_3^{2-}. The excessive CO_3^{2-} reacted with Ca^{2+} in the solution to produce more $CaCO_3$, thus lowing the overall Mg^{2+}/Ca^{2+} ratio.

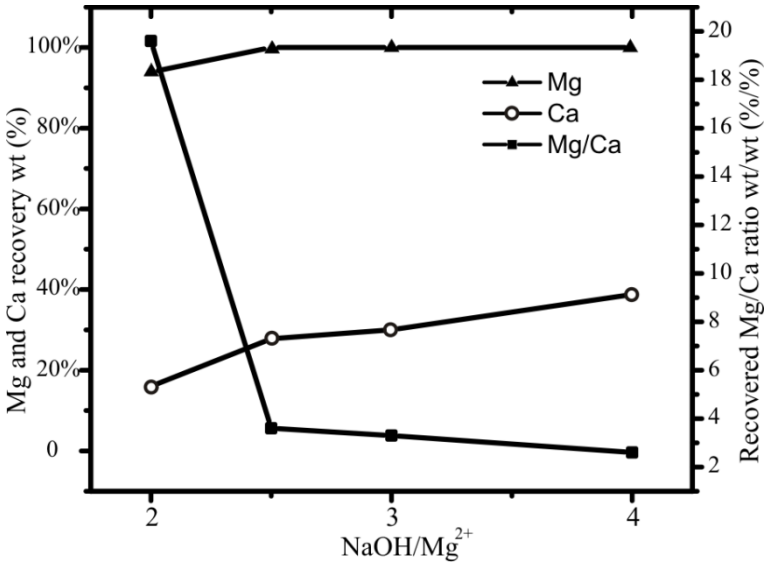

Figure 2 Percentage of Mg^{2+} and Ca^{2+} sequestrated from reject brine as a function of the $NaOH/Mg^{2+}$ molar ratio

3.2 Characterization of the synthesized $Mg(OH)_2$

3.2.1 XRD

Figure 3 shows the XRD diffractograms of $Mg(OH)_2$ obtained from the reaction of reject brine and NaOH at different $NaOH/Mg^{2+}$ molar ratios. The diffraction patterns of all samples demonstrated the presence of $Mg(OH)_2$ along with $CaCO_3$. A shift in the crystal structure of $CaCO_3$ from aragonite to calcite was observed at increased $NaOH/Mg^{2+}$ ratios. This could be attributed to the presence of Mg^{2+} in brine, which inhibited the precipitation of calcite and favored the formation of aragonite at low $NaOH/Mg^{2+}$ ratios [43]. Alternatively, the high pH of the solution at elevated $NaOH/Mg^{2+}$ ratios, at which the influence of Mg^{2+} was minimal, favored the formation of calcite.

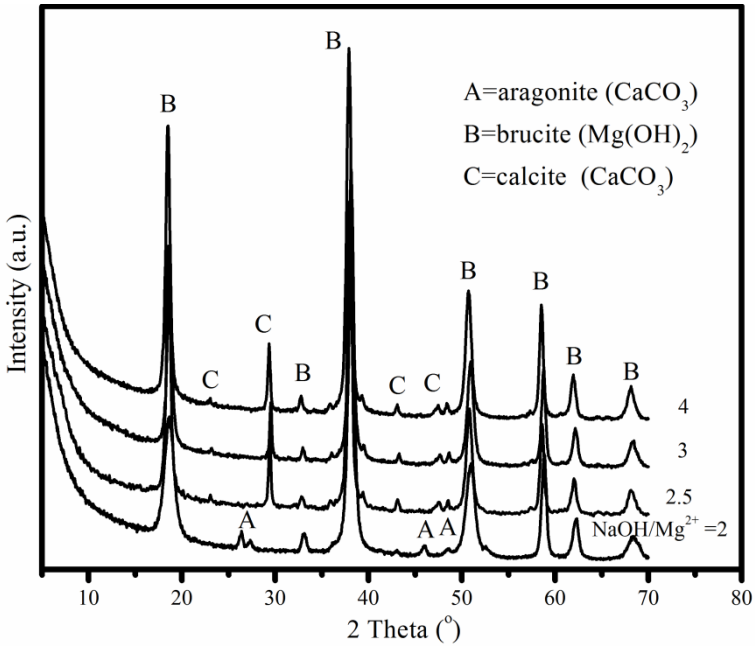

Figure 3 XRD diffractograms of $Mg(OH)_2$ obtained from the reaction of reject brine with NaOH at different $NaOH/Mg^{2+}$ molar ratios

3.2.2 FESEM

The morphologies of $Mg(OH)_2$ samples obtained at different $NaOH/Mg^{2+}$ molar ratios were investigated by FESEM, as shown in Figure 4. A plate-like morphology was observed at a $NaOH/Mg^{2+}$ ratio of 2. The morphology of $Mg(OH)_2$ transformed into a granular pattern consisting of a denser structure at increased $NaOH/Mg^{2+}$ ratios, which could be due to the increased pH of the solution. This was because higher pH values led to the generation of higher concentrations of OH^- in the solution. The increased availability of OH^- accelerated the nucleation of $Mg(OH)_2$ crystals and enabled the formation of larger amounts of $Mg(OH)_2$, facilitating the densification of the overall structure.

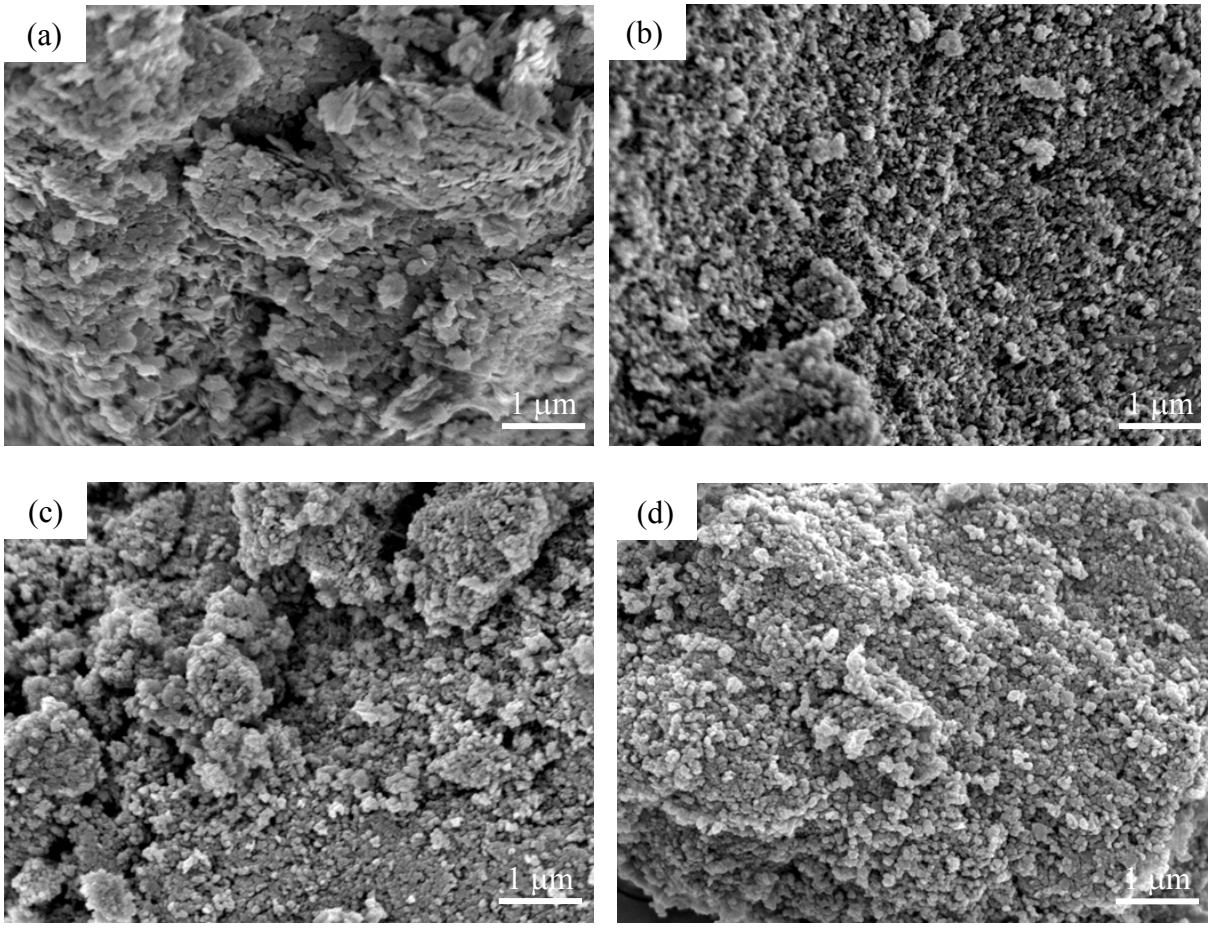

Figure 4 FESEM images of $Mg(OH)_2$ obtained from the reaction of reject brine with NaOH at different NaOH/Mg^{2+} molar ratios of (a) 2, (b) 2.5, (c) 3 and (d) 4

3.2.3 TG/DTA

Figure 5 illustrates a typical TG/DTA graph of $Mg(OH)_2$ obtained via the reaction of brine with NaOH at a NaOH/Mg^{2+} molar ratio of 2. The dehydration of $Mg(OH)_2$ took place at ~400 °C and resulted in a mass loss of around 24.2%, which was attributed to the loss of water. The decomposition patterns observed during TG/DTA were in line with previous studies that investigated the decomposition of $Mg(OH)_2$ into MgO [24, 26-28, 30, 32]. The second endothermic peak, observed at ~720 °C, was due to the decarbonation of $CaCO_3$. The decomposition of $CaCO_3$ led to the release of CO_2, resulting in a mass loss of around 2.3%.

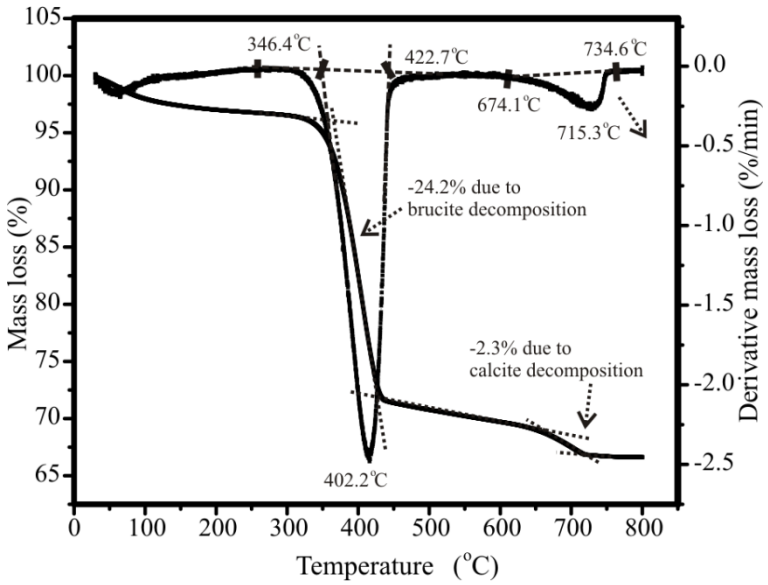

Figure 5 A typical TG/DTA curve of $Mg(OH)_2$ obtained from the reaction of reject brine at a $NaOH/Mg^{2+}$ molar ratio of 2

Table 2 summarizes the TG/DTA results of $Mg(OH)_2$ obtained from the reaction of brine with NaOH at various $NaOH/Mg^{2+}$ ratios ranging between 2 and 4. The results show that the mass loss due to dehydration of $Mg(OH)_2$ at ~400 °C slightly decreased (24.2 to 22.6%), while the mass loss due to decarbonation of $CaCO_3$ at ~720 °C slightly increased (2.3 to 3.9%) with increasing $NaOH/Mg^{2+}$ ratios. This was mainly attributed to the increased content of $CaCO_3$ in the precipitates at higher $NaOH/Mg^{2+}$ ratios, which was in line with the findings shown in Figure 2.

Table 2 TG/DTA results of the decomposition of $Mg(OH)_2$ obtained from the reaction of reject brine with NaOH at different $NaOH/Mg^{2+}$ ratios

Mg^{2+}/ NaOH	Peak temperature (°C)	Mass loss between 340-440 °C (%)	Peak temperature (°C)	Mass loss between 650-750 °C (%)
1:2	402.2	24.2	715.3	2.3
1:2.5	401.2	23.5	721.1	3.2
1:3	400.8	23.3	719.3	3.5
1:4	404.1	22.6	724	3.9

Table 3 compares the compositions of the synthesized $Mg(OH)_2$ based on the TG/DTA (Table 2) and the ICP-OES (Figure 2) results. Both measurements revealed similar trends, showing a decrease in the mass percentage of $Mg(OH)_2$, accompanied with an increase in the mass percentage of $CaCO_3$ (and thus a decrease in the purity of precipitates) with increasing NaOH/Mg^{2+} molar ratios, which was further discussed in Section 3.1. Accordingly, the highest amount of $Mg(OH)_2$ (93.7% by TGA and 95.4% by ICP-OES) was synthesized at a NaOH/Mg^{2+} molar ratio of 2. Therefore, this ratio was chosen as the optimum condition for the subsequent production and characterization of reactive MgO.

Table 3 Composition of synthesized $Mg(OH)_2$ based on TG/DTA and ICP-OES results

Mg^{2+}/NaOH	TG/DTA		ICP-OES	
	$Mg(OH)_2$ (%)	$CaCO_3$ (%)	$Mg(OH)_2$ (%)	$CaCO_3$ (%)
1:2	93.7	6.3	95.4	4.6
1:2.5	91.2	8.8	91.2	8.8
1:3	90.4	9.6	90.6	9.4
1:4	89.2	10.8	88.1	11.9

3.3 Characterization of the synthesized reactive MgO

3.3.1 SSA

Figure 6 presents the SSA of the reactive MgO obtained under different calcination conditions. In general, SSA reduced with increasing calcination temperature and duration, which was in line with the findings of previous studies [24, 26-28, 30, 32]. This was associated with the sintering and agglomeration of MgO grains at higher temperature and prolonged residence times. In the current study, the highest SSA of 51.4 m^2/g was obtained when the synthesized $Mg(OH)_2$ was calcined at 500 ^oC for 2 hours. When compared to other studies, the SSA value (51.4 m^2/g) obtained under these conditions was significantly higher than the results presented in the literature, where MgO synthesized from a magnesium

chloride solution via the addition of NaOH and calcined under the same conditions (i.e. 500 ^{o}C for 2 hours), was reported to possess a SSA of 22.1 m^2/g [44]. However, compared with our previous study, MgO calcined at 500 °C for 2 hours from reject brine via the addition of NH_4OH showed a higher SSA of 78.8 m^2/g [31]. This could be because the use of NaOH as the alkali source was found to form $Mg(OH)_2$ with a globular cauliflower-like morphology; while the use of NH_4OH resulted in a more porous plate-like morphology [31]. A relative more porous mother precursor would result in a more porous MgO, thus a higher reactivity. These values can be optimized even further with an adjustment of the calcination temperature and duration towards the lower range, while enabling the complete decomposition of $Mg(OH)_2$.

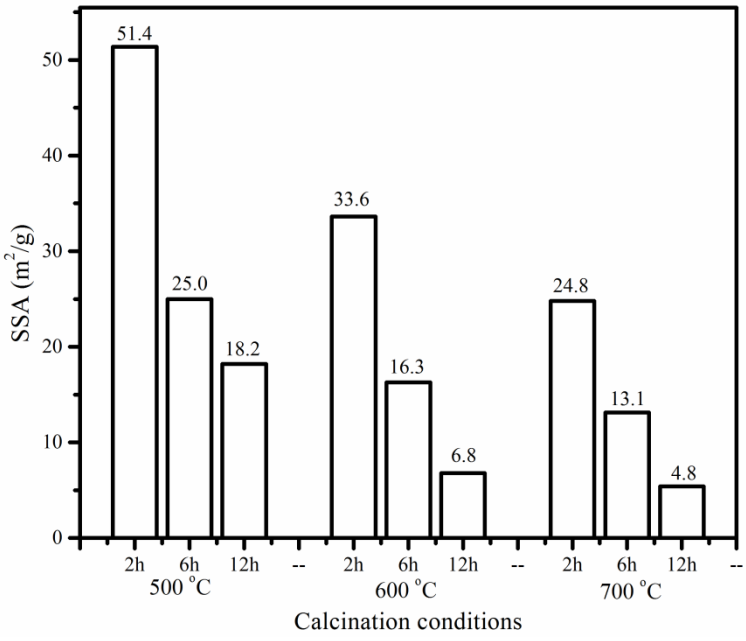

Figure 6 SSA of MgO produced under different calcination temperatures and durations

3.3.2 Reactivity

Figure 7 shows the acid reactivity of MgO obtained under different calcination conditions. An increase in the neutralization time was observed with increasing calcination temperature

and duration, which reflected the reduction in the reactivity of MgO. This observation corresponded well with the SSA measurements reported earlier in Figure 6. A comparison of the reactivity and SSA of MgO is shown in Figure 8, where the inverse correlation between the two parameters was revealed. Accordingly, MgO samples with higher SSA resulted in shorter acid neutralization times, which was an indication of their higher reactivities. These findings were in line with those reported in earlier studies [12, 30], where a direct correlation between the SSA and reactivity of MgO was reported.

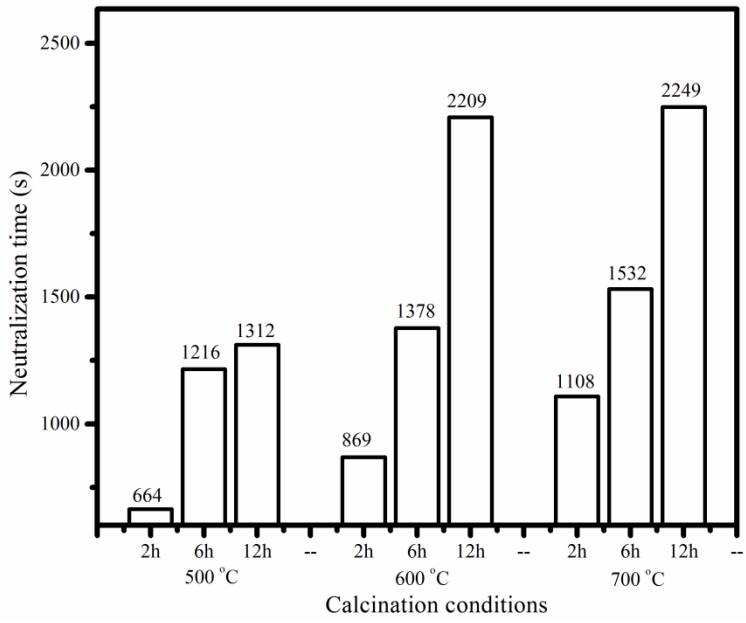

Figure 7 Effect of calcination temperature and duration on the reactivity of MgO

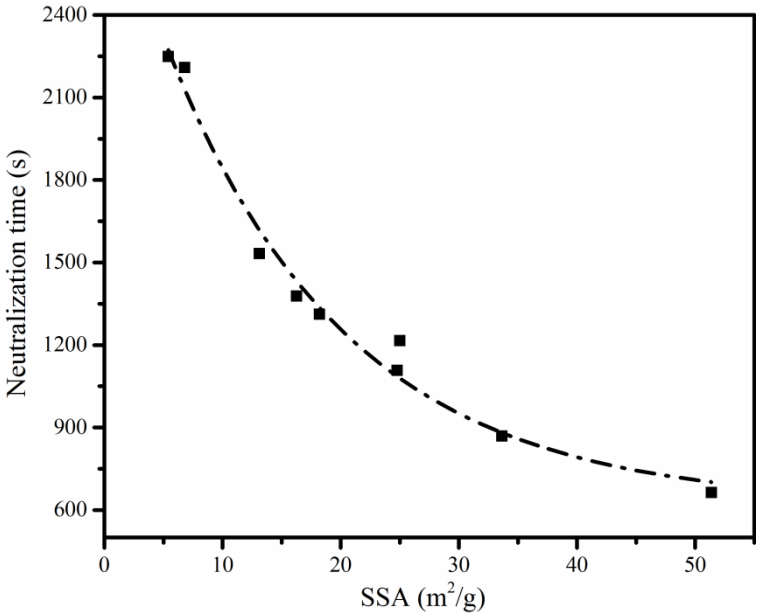

Figure 8 Relationship between the SSA and the reactivity of MgO

3.3.3 XRD

Figure 9 illustrates the diffractograms of MgO obtained via the calcination of $Mg(OH)_2$, which was synthesized at a $NaOH/Mg^{2+}$ molar ratio of 2. The main peak positions of the synthesized MgO were located at ~37.0°, 42.9° and 62.3° 2θ, which matched well with the reference peaks of MgO indicated in JCPDS card no. 89-7746. These peaks were accompanied with a few minor peaks attributed to $CaCO_3$. The absence of $Mg(OH)_2$ peaks indicated the complete decomposition of brucite under the calcination conditions adopted in this study. Aragonite, which was initially present along with $Mg(OH)_2$, transformed into calcite at higher calcination temperatures of 600 °C [45]. A further increase in the calcination temperature (700 °C) and duration led to a reduction in the intensity of the calcite peaks due to decomposition of $CaCO_3$.

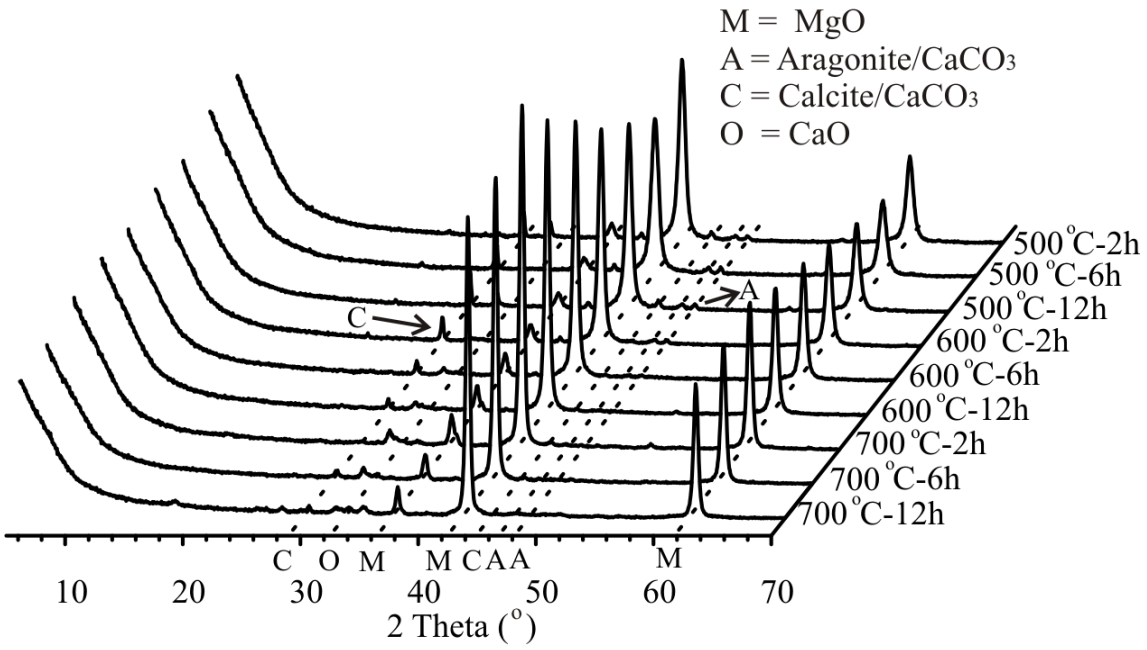

Figure 9 XRD diffractograms of reactive MgO produced via the calcination of $Mg(OH)_2$ under different temperatures and durations

3.3.4 FESEM

A further investigation on the influence of calcination temperature and duration on the SSA of MgO was revealed through FESEM. The changes in the microstructure of MgO at increased temperatures and durations are indicated in Figure 10, which is a good indication of the typical morphology of MgO produced at a calcination temperature of 500-700 °C and a residence time of 2-12 hours. The microstructure of MgO was composed of a single particle which was a combination of several grains. A plate-like morphology, which was inherited from the parent material ($Mg(OH)_2$), was observed throughout the microstructure of MgO produced at lower temperatures. An increase in the particle size, accompanied with the creation of a more porous structure, was observed at increased temperatures and durations. The loss of water during the decomposition of $Mg(OH)_2$ led to the formation of a porous structure, which gradually reduced with the increase in the size of the MgO grains due to continued sintering, causing a reduction in the total pore volume.

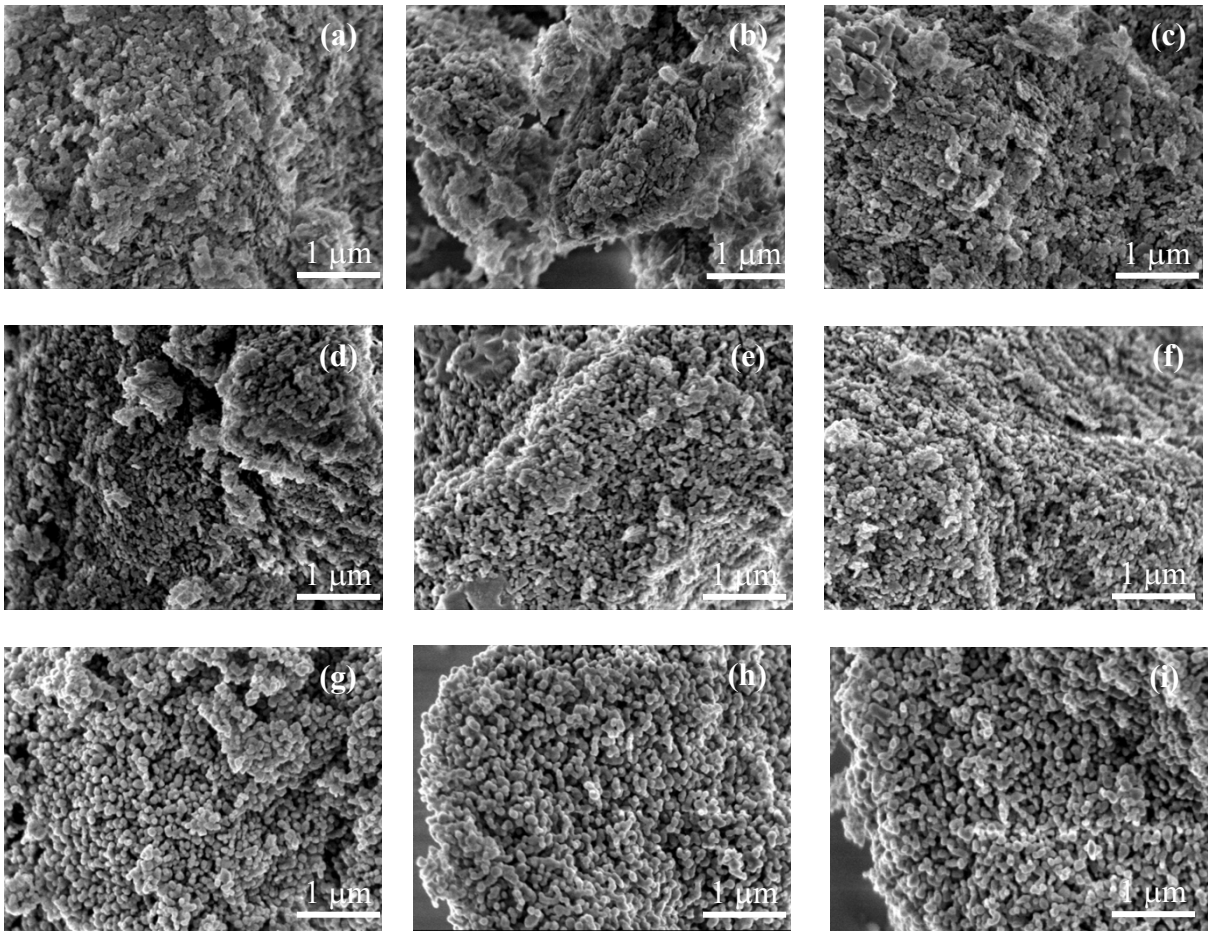

Figure 10 FESEM images of MgO obtained from the calcination of $Mg(OH)_2$ under different conditions: (a) 500°C-2h, (b) 500°C-6h, (c) 500°C-12h, (d) 600°C-2h, (e) 600°C-6h, (f) 600°C-12h, (g) 700°C-2h, (h) 700°C-6h and (i) 700°C-12h

3.4 Economic feasibility

The costs of the production of reactive MgO from reject brine via the addition of NaOH, NH_3, or CaO were calculated and compared. In the first step, base is added into reject brine to precipitate $Mg(OH)_2$. Raw material costs of NaOH, NH_3, and CaO are reported to be ~S$571/ton NaOH [46], ~S$525/ton NH_3 [47], and ~S$170/ton CaO [48], respectively. Cost of reject brine, transportation of raw materials, and grinding and packing of reactive MgO are not considered. Since a production yield of 1 ton reactive MgO requires 2 tons NaOH, 1 ton

373 NH_3, or 1.4 ton CaO as the base source, the raw material costs are calculated to be
374 S$1142/ton MgO, S$525/ton MgO and S$238/ton MgO via the addition of NaOH, NH_3, or
375 CaO, respectively.
376
377 The resulting $Mg(OH)_2$ produced in the first step was in the form of filter cake which consists
378 of 55.2% solids and 44.8% free water. In the second step, $Mg(OH)_2$ filter cake was calcinated
379 to produce MgO. Energy consumption during calcination of $Mg(OH)_2$ filter cake is derived
380 by considering the following two steps: (i) Energy consumed to increase the temperature
381 from room temperature (298 K, 25 °C) to the decomposition temperature of $Mg(OH)_2$ (773K,
382 500 °C), and (ii) enthalpy of decomposition of $Mg(OH)_2$ [3]. A production yield of 1 ton
383 MgO requires decomposing 1.45 ton $Mg(OH)_2$ and the decomposition temperature of
384 $Mg(OH)_2$ under one atmosphere CO_2 pressure is in the range between 773 and 973 K (500
385 and 700 °C). Firstly the energy required to raise the temperature from ambient air (298 K) to
386 the decomposition temperature (773 K) is calculated using the formula: C_p × increase in
387 temperature (K). The specific heat capacity (C_p) of $Mg(OH)_2$ at 773 K is 1.78 kJ/kg K, which
388 results in the energy demand of 1.15 GJ in consideration of the purity of the synthesized
389 $Mg(OH)_2$ of ~94%. The energy required for decomposition of $Mg(OH)_2$ is calculated based
390 on the enthalpy of decomposition (1304 kJ/kg K), which brings in 1.77 GJ. As for the free
391 water, energy required to increase temperature of free water from room temperature (298 K)
392 to the boiling point (373 K) is calculated based on the specific heat capacity of water (4.18
393 kJ/kg K) and the percentage of water in the filter cake (44.8%), resulting in 0.37 GJ. This is
394 followed by the enthalpy of the vaporization of water (2283 kJ/kg K), resulting in 2.69 GJ.
395 Finally the energy required to heat up the resultant steam to 773 K is calculated via the heat
396 capacity of water vapour (1.86 kJ/kg K), bringing in 0.88 GJ. The total energy required for
397 the calcination process is the summation of the energy required for each individual step,

resulting in a total of 6.85 GJ (1902.8 kWh) for the production of 1 ton reactive MgO from reject brine via the addition of base. As of 2015, Singapore uses natural gas (95%) and others (4%) for the power generation at a price of 20.2 cents per kWh [49], which results in an energy cost of S$384 to product 1 ton reactive MgO from reject brine via the addition of a base.

Production cost of the resulting MgO via the addition of NaOH, NH_3, and CaO in reject brine are S$1526, S$909, and S$622 per ton MgO, respectively, as shown in Figure 11. Price of MgO produced via a dry route in the US market was reported to be S$617 per ton MgO [50]. Thus, a cheaper base alternative would make the production of reactive MgO from reject brine more economically feasible. Furthermore, synthetic MgO from reject brine shows a much higher purity and reactivity compared to the dry route as the SSA of commercial MgO is usually ~20 m^2/g [3], which makes synthetic MgO more competitive in the global market.

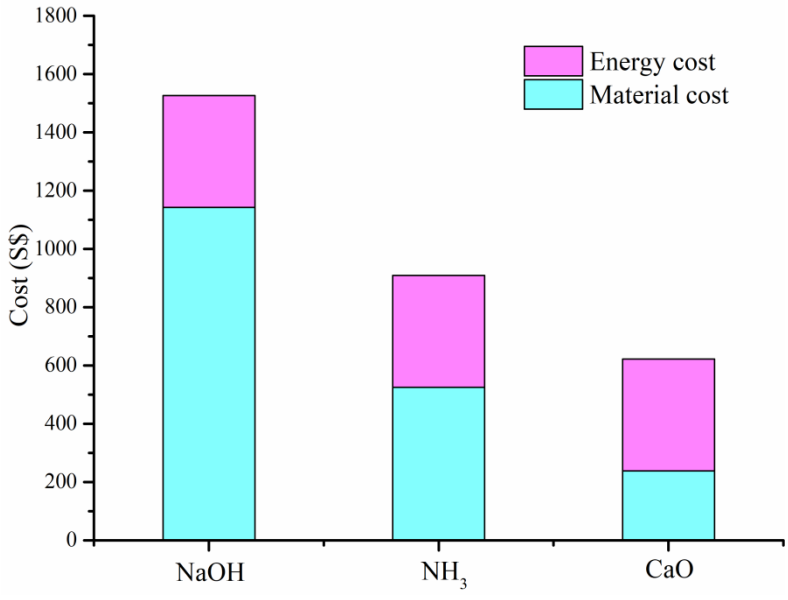

Figure 11 Production cost of reactive MgO from reject brine via the addition of NaOH, NH_3, or CaO.

4 Conclusions

This study presented a comprehensive investigation on the synthesis of $Mg(OH)_2$ and production of reactive MgO from reject brine via the use of NaOH. The key parameters affecting the properties of the synthesized $Mg(OH)_2$ and its calcination to produce reactive MgO were revealed. The results demonstrated the feasibility of recovering reactive MgO from reject brine obtained as a waste at the end of the desalination process. The initial set of experiments successfully demonstrated the use of NaOH as an alkali source in the precipitation of $Mg(OH)_2$ from reject brine. The effect of the $NaOH/Mg^{2+}$ ratio on the final yield was investigated with the goal of optimizing the amount and purity of the synthesized $Mg(OH)_2$. An optimum $NaOH/Mg^{2+}$ ratio of 2, which generated the highest purity of $Mg(OH)_2$, was determined and used in the subsequent production of MgO. The influence of calcination conditions (i.e. temperature and residence time) on the reactivity of MgO obtained via the calcination of the synthesized $Mg(OH)_2$ were reported. While a certain minimum temperature was required for the complete decomposition of $Mg(OH)_2$ into MgO, an increase in the calcination temperature and duration lowered the reactivity of MgO. Calcination of $Mg(OH)_2$ at 500 ºC for 2 hours resulted in the most reactive MgO samples, with a SSA of 51.4 m^2/g. This study demonstrated that reject brine can be considered as a feasible and economic alternative source for the sustainable recovery of MgO with a high reactivity, which can be used in various applications within the food, cosmetics, pharmaceutical and construction industries [1-3].

Acknowledgement

This project is funded by the National Research Foundation (NRF), Prime Minister's Office, Singapore under its Campus for Research Excellence and Technological Enterprise (CREATE) program. Special thanks to Ms. Rui Hao for her review and comments of the

441 manuscript.

442

444 **References**

445 [1] D.A. Kramer, Magnesium, its alloys and compounds, Industrial Minerals and Rocks,
446 2001.

447 [2] E.K. Lee, K.D. Jung, O.S. Joo, Y.G. Shul, Magnesium oxide as an effective catalyst in
448 catalytic wet oxidation of H2S to sulfur, Reaction Kinetics and Catalysis Letters, 82, 2004,
449 241-246.

450 [3] M.A. Shand, The chemistry and technology of magnesia, 2006.

451 [4] M.A. Caraballo, T.S. Rotting, F. Macias, J.M. Nieto, C. Ayora, Field multi-step limestone
452 and MgO passive system to treat acid mine drainage with high metal concentrations, Applied
453 Geochemistry, 24, 2009, 2301-2311.

454 [5] L.W. Mo, M. Deng, M.S. Tang, A. Al-Tabbaa, MgO expansive cement and concrete in
455 China: Past, present and future, Cement and Concrete Research, 57, 2014, 1-12.

456 [6] A.J.W. Harrison, Reactive magnesium oxide cements, 2008.

457 [7] M. Liska, A. Al-Tabbaa, K. Carter, J. Fifield, Scaled-up commercial production of
458 reactive magnesium cement pressed masonry units. Part I: Production, Proceedings of the
459 Institution of Civil Engineers-Construction Materials, 165, 2012a, 211-223.

460 [8] M. Liska, A. Al-Tabbaa, K. Carter, J. Fifield, Scaled-up commercial production of
461 reactive magnesia cement pressed masonry units. Part II: Performance, Proceedings of the
462 Institution of Civil Engineers-Construction Materials, 165, 2012b, 225-243.

463 [9] C. Unluer, A. Al-Tabbaa, Impact of hydrated magnesium carbonate additives on the
464 carbonation of reactive MgO cements, Cement and Concrete Research, 54, 2013, 87-97.

465 [10] C. Unluer, A. Al-Tabbaa, Enhancing the carbonation of MgO cement porous blocks
466 through improved curing conditions, Cement and Concrete Research, 59, 2014, 55-65.

467 [11] A. Al-Tabbaa, Reactive magnesia cement, in: F. PachecoTorgal, S. Jalali, J. Labrincha,
468 V.M. John (Eds.) Eco-Efficient Concrete, 2013, pp. 523-543.

469 [12] F. Jin, A. Al-Tabbaa, Characterisation of different commercial reactive magnesia,
470 Advances in Cement Research, 26, 2014, 101-113.
471 [13] Y. Soong, A.L. Goodman, J.R. McCarthy-Jones, J.P. Baltrus, Experimental and
472 simulation studies on mineral trapping of CO2 with brine, Energy Conversion and
473 Management, 45, 2004, 1845-1859.
474 [14] M.L. Druckenmiller, M.M. Maroto-Valer, Carbon sequestration using brine of adjusted
475 pH to form mineral carbonates, Fuel Processing Technology, 86, 2005, 1599-1614.
476 [15] R. Hao, Investigation into the Production of Carbonates and Oxides from Synthetic
477 Brine through Carbon Sequestration, in: Department of Engineering, University of
478 Cambridge, 2017.
479 [16] R. Friedrich, H. Robinson, R. Spencer, Magnesium hydroxide from sea water, in,
480 Google Patents, 1946.
481 [17] N. Petric, V. Martinac, M. Labor, The effect of mannitol and pH of the solution on the
482 properties of sintered magnesium oxide obtained from sea water, Chemical Engineering &
483 Technology, 20, 1997, 36-39.
484 [18] M. Turek, W. Gnot, Precipitation of magnesium hydroxide from brine, Industrial &
485 Engineering Chemistry Research, 34, 1995, 244-250.
486 [19] R.H. Dave, P.K. Ghosh, Enrichment of bromine in sea-bittern with recovery of other
487 marine chemicals, Industrial & Engineering Chemistry Research, 44, 2005, 2903-2907.
488 [20] M.H. El-Naas, Reject brine management, in: Desalination, trends and technologies,
489 InTech, 2011, pp. 237-252.
490 [21] K.T. Tran, T. Van Luong, J.W. An, D.J. Kang, M.J. Kim, T. Tran, Recovery of
491 magnesium from Uyuni salar brine as high purity magnesium oxalate, Hydrometallurgy, 138,
492 2013, 93-99.

493 [22] T. Khuyen Thi, K.S. Han, S.J. Kim, M.J. Kim, T. Tam, Recovery of magnesium from
494 Uyuni salar brine as hydrated magnesium carbonate, Hydrometallurgy, 160, 2016, 106-114.
495 [23] S. Casas, C. Aladjem, E. Larrotcha, O. Gibert, C. Valderrama, J.L. Cortina, Valorisation
496 of Ca and Mg by-products from mining and seawater desalination brines for water treatment
497 applications, Journal of Chemical Technology and Biotechnology, 89, 2014, 872-883.
498 [24] W.R. Eubank, Calcination studies of magnesium oxides, Journal of the American
499 Ceramic Society, 34, 1951, 225-229.
500 [25] J. Green, Calcination of precipitated Mg (OH) 2 to active MgO in the production of
501 refractory and chemical grade MgO, Journal of Materials Science, 18, 1983, 637-651.
502 [26] K. Itatani, K. Koizumi, F.S. Howell, A. Kishioka, M. Kinoshita, Agglomeration of
503 magnesium oxide particles formed by the decomposition of magnesium hydroxide .1.
504 Agglomeration at increasing temperature, Journal of Materials Science, 23, 1988, 3405-3412.
505 [27] V. Choudhary, V. Rane, R. Gadre, Influence of precursors used in preparation of MgO
506 on its surface properties and catalytic activity in oxidative coupling of methane, Journal of
507 Catalysis, 145, 1994, 300-311.
508 [28] E. Alvarado, L.M. Torres-Martinez, A.F. Fuentes, P. Quintana, Preparation and
509 characterization of MgO powders obtained from different magnesium salts and the mineral
510 dolomite, Polyhedron, 19, 2000, 2345-2351.
511 [29] I.F. Mironyuk, V.M. Gun'ko, M.O. Povazhnyak, V.I. Zarko, V.M. Chelyadin, R.
512 Leboda, J. Skubiszewska-Zięba, W. Janusz, Magnesia formed on calcination of Mg(OH)2
513 prepared from natural bischofite, Applied Surface Science, 252, 2006, 4071-4082.
514 [30] L.W. Mo, M. Deng, M.S. Tang, Effects of calcination condition on expansion property
515 of MgO-type expansive agent used in cement-based materials, Cement and Concrete
516 Research, 40, 2010, 437-446.

517 [31] H. Dong, C. Unluer, E.-H. Yang, A. Al-Tabbaa, Synthesis of reactive MgO from reject
518 brine via the addition of NH_4OH, Hydrometallurgy, 169, 2017, 165-172.
519 [32] J.K. Bartley, C. Xu, R. Lloyd, D.I. Enache, D.W. Knight, G.J. Hutchings, Simple
520 method to synthesize high surface area magnesium oxide and its use as a heterogeneous base
521 catalyst, Applied Catalysis B: Environmental, 128, 2012, 31-38.
522 [33] L.F. Greenlee, D.F. Lawler, B.D. Freeman, B. Marrot, P. Moulin, Reverse osmosis
523 desalination: water sources, technology, and today's challenges, Water research, 43, 2009,
524 2317-2348.
525 [34] C. Fritzmann, J. Lowenberg, T. Wintgens, T. Melin, State-of-the-art of reverse osmosis
526 desalination, Desalination, 216, 2007, 1-76.
527 [35] ST, Fifth Singapore desalination plant in the pipeline, in, The Straits Times, The Straits
528 Times, 2016.
529 [36] IDA, The current state of desalination, in, International Desalination Association, 2015.
530 [37] S. Adham, A. Hussain, J.M. Matar, R. Dores, A. Janson, Application of Membrane
531 Distillation for desalting brines from thermal desalination plants, Desalination, 314, 2013,
532 101-108.
533 [38] A.M.O. Mohamed, M. Maraqa, J. Al Handhaly, Impact of land disposal of reject brine
534 from desalination plants on soil and groundwater, Desalination, 182, 2005, 411-433.
535 [39] M.H. El-Naas, A.H. Al-Marzouqi, O. Chaalal, A combined approach for the
536 management of desalination reject brine and capture of CO2, Desalination, 251, 2010, 70-74.
537 [40] D.H. Kim, A review of desalting process techniques and economic analysis of the
538 recovery of salts from retentates, Desalination, 270, 2011, 1-8.
539 [41] M. Elimelech, W.A. Phillip, The Future of Seawater Desalination: Energy, Technology,
540 and the Environment, Science, 333, 2011, 712-717.

[42] L.G. Sillen, A.E. Martell, J. Bjerrum, Stability constants of metal-ion complexes, Chemical Society London, 1964.

[43] R.A. Berner, The role of magnesium in the crystal growth of calcite and aragonite from sea water, Geochimica et Cosmochimica Acta, 39, 1975, 489-504.

[44] T.G. Venkatesha, R. Viswanatha, Y.A. Nayaka, B.K. Chethana, Kinetics and thermodynamics of reactive and vat dyes adsorption on MgO nanoparticles, Chemical Engineering Journal, 198, 2012, 1-10.

[45] C.G. Kontoyannis, N.V. Vagenas, Calcium carbonate phase analysis using XRD and FT-Raman spectroscopy, The Analyst, 125, 2000, 251-255.

[46] Y. Fukushima, Caustic soda prices on upward trend in Asian markets, 2016.

[47] A. Jones, Why do ammonia prices keep falling?, 2016.

[48] USGS, Minerals yearbook-lime 2012, 2012.

[49] EMA, Singapore energy statistics 2016, Energy Market Authority, 2016.

[50] S. Bogner, MGX minerals plans to enter the magnesium market in 2016, Rockstone Reserach Ltd., 2015.